IS-T 1765

Amperometric Detection and Electrochemical Oxidation of Aliphatic Amines and Ammonia on Silver-lead Oxide Thin-film Electrodes

by

Ge, Jisheng

PHD Thesis submitted to Iowa State University

Ames Laboratory, U.S. DOE

Iowa State University

Ames, Iowa 50011

Date Transmitted: January 8, 1996

PREPARED FOR THE U.S. DEPARTMENT OF ENERGY

UNDER CONTRACT NO. W-7405-Eng-82.

DISCLAIMER

DEDICATION

To my wife, Xiaobing, who has provided me with love, spiritual and family support and especially brought me a beautiful son during my unforgettable staying in Ames.

TABLE OF CONTENTS

GENERAL INTRODUCTION

Dissertation Organization

This dissertation contains three published or submitted papers in internationally acknowledged journals. Each paper consists of separate abstract, introduction, experimental, results and discussion, conclusion and acknowledgement respectively. Preceding the body of three papers is this general introduction and following is a general conclusion and acknowledgement. The reference citations of general introduction and general conclusion are listed at the end of this dissertation.

This research project was started at 1992 under direction of Professor Dennis C. Johnson for partial fulfillment of the degree of doctor of philosophy of Iowa State University. The first paper describes the discovery of electrocatalytic activity of silver-lead oxide thin-film electrodes for anodic oxidation of aliphatic amines. Also included are experimental details and data interpretation of electrode fabrication, activity testing by cycle voltammetry and amperometry, and physical and chemical characterization of oxide surface. The application of the electrode in flow system detection such as flow injection analysis is described also. A perceptive mechanism of electrocatalytic activity in terms of hydroxyl radical formation on electrode surface is discussed.

The second paper describes electrochemical anodic oxidation of ammonia on anodized eutectic phase Ag-Pb alloy electrode by applied potentials in either triangle waveforms such as in voltammetry or constant forms such as in exhaustive electrolysis. Paper gives experimental results and the methods used in separation, detection, and

determination of oxidation products in electrolysis solution. A stepwise reaction pathway for the oxidation of aliphatic amines especially ethylamine is proposed based on comparison of heterogenous electron transfer rate constants of ethylamine and ammonia.

In the third paper, the main focus is on temperature effects of anodic oxidation of ethylamine, alanine and ammonia at anodized eutectic phase Ag-Pb alloy electrodes. A follow-through reactor interfaced with ion chromatography (IC) is specially designed and set up for the measurement of oxidation products of extremely volatile ammonia at elevated temperatures. The activation energies of the anodic oxidation of ethylamine, alanine and ammonia are estimated based on these experimental data. Typically, large efforts are made on interpretation of anodic oxidation mechanisms in terms of oxygen transfer through incorporation of surface adsorbed hydroxyl radicals by linear correlation of net peak potentials, logarithm of heterogenous rate constants with overpotentials of oxygen evolution.

Amines, Ammonia and Their Importance

An amine has general formula RNH_2, R_2NH, or R_3N, where R is any alkyl or aryl group. Amines are classified as primary, secondary, and tertiary amines according to the number of groups attached to the nitrogen atom. When R is an alkyl group the amine is called aliphatic amine. Particularly when R is replaced by hydrogen atom (H), the molecule is called ammonia and classified as inorganic compound. From this point of view, any amine can be considered as an analog of ammonia by replacing one or more hydrogen atoms with organic alkyl or aryl groups.

Amine is a very basic and important organic functional group which widely exists in nature in a great variety of substances. Many of these substances are key compounds in living organisms. For example, amino acids are the main structure unit of protein and enzyme, biogenic amines such as catecholamine and dopamine are essential information transmitters in human central nervous systems. In many industrial areas, amine compounds have found widespread applications such as corrosion control, metal surface finishing, and emulsifying agents, the manufacturing of laundry additives and dyes, and in rubber stabilizers [1,2]. Amine groups are also common structure moiety in synthetic pharmaceutical chemicals based on structure-function relationship studies of their natural analogies [3]. Short chain aliphatic amines and simple aromatic amines are also starting synthetic materials in chemical industries [4]. Naturally existing ammonia takes a very important part in environmental nitrogen cycles such as nitrification, ammonification, assimilation, and biological nitrogen fixation [5]. Synthetic ammonia plays a very important role in chemical industry for production of fertilizers, explosives, and also nitric acid through so-called Ostwald oxidation process [6].

Analysis and Detection of Aliphatic Amines

Due to extensive existence in nature and increasingly contact with human beings, chemical analysis and determination of aliphatic amines have become a routine practice in chemical, biological, pharmaceutical and environmental protection and waste control industries and laboratories. Aliphatic amines and ammonia are optically inert in nature. The existence of lone electron pairs on nitrogen atom bears aliphatic amines and ammonia

the characteristics of very polar, hydrophilic and highly soluble in aqueous solution. These typical physical chemical properties made their detection even more difficult. For example, conventional techniques such as photometry by absorption or luminescence and gas chromatography (GC) are not directly available because of lack of chromophores and high hydrophilicity. Detection of aliphatic amines by refractive index with liquid chromatographic separation is possible but sensitivity is limited because refractive index is a direct function of temperature [7]. Detection and analysis of aliphatic amines by other techniques such as fourier transfer infra-red spectroscopy (FTIR) [8], nuclear magnetic resonance (NMR) [9], and mass spectrometry (MS) [10] are not routinely used except in extreme conditions, because the techniques are featured by less sensitive (FTIR, NMR), high cost (NMR and MS), poor resolution (FTIR) and time-consuming sample preparation involved. Through derivatization with chromophores, volatile groups and chemiluminescence reagents, the detection and analysis of aliphatic amines and amino acids by high performance liquid chromatography (HPLC) [11] with photometric detection or by gas chromatography [12] are possible. These techniques are also limited in practical usage because of poor quantification, judicious choice of derivertizing reagent, time-consuming derivertizing step and troublesome in final cleanup of the waste. It is appropriate to expect that uncover a more reliable, easy to operate and sensitive detection scheme for these optically inert compounds is becoming more and more compelling task for analytical chemists.

Merit of Electrochemical Analysis and Detection

Most of the analytical techniques are designed based on information transfer by transducer or detection mechanism from directly sensed physical, chemical and biological property changes of analyte in a complex matrix or medium to electrical signals such as potential, current, conductivity and capacity. Electrochemical detection is perhaps the only technique that can directly acquire electrical signals from analytes in a complex matrix or media. The combination advantages of simplicity, sensitivity, and easy operation have made electrochemical detection a very attractive and promising analytical technique in variety of industrial applications.

Very often electrochemical phenomena are taking place between solid (electrochemical transducer or electrode) and liquid (supporting electrolyte and analyte) interface such as in battery, fuel cell, in vitro or in vivo electrochemical sensor, and corrosion processes. In depth understanding of the interfacial chemistry between solid electrode and liquid phase especially aqueous solution will undoubtedly provide powerful directing tools in design, fabrication, operation and control of transducing electrodes for specific purpose of application. A usful electrochemical transducer for amperometric detection requires electrode possessing extraordinary interfacial characteristics such as (i) good electrical conductivity to ensure continuous flow of electron current, (ii) general electrolyte compatibility with corrosion resistance to maintain electrode stability, (iii) with catalytic activity to promote infinite large kinetic rate of any pre- or post-chemical reaction to generate sensitive limiting current signals, (iv) less toxicity or bio-compatibility for in vivo application, and (v) analyte selectivity for eliminating unnecessary

eliminating unnecessary interferences. Some characteristic factors may be more demanding than others depending on applications and technical requirements.

Electrochemical Detection of Aliphatic Amines

Aliphatic amines are highly polar and hydrophilic organics commonly existing in aqueous solutions. Many efforts have be made in devising a direct detection scheme for aliphatic amines in aqueous solution but electrochemical detection is very notable. In organic functional group redox series, amine is in very reductive end and easily to be oxidized by looking at following:

$$\underset{}{R\text{-}CN} \overset{\substack{-4e \\ -H^+}}{\leftarrow} \underset{}{R\text{-}NH_2} \overset{\substack{H_2O \\ NH_3}}{\rightleftarrows} \underset{}{R\text{-}OH} \overset{\substack{-2e \\ -H^+}}{\rightarrow} \underset{}{R\text{-}CHO(=CO)} \overset{\substack{-2e \\ -H^+}}{\rightarrow} \underset{}{R\text{-}COOH} \overset{\substack{Heat \\ H_2O}}{\rightarrow} \underset{}{CO_2} \qquad (1)$$

General considerations in electrochemical detection or more specifically amperometric detection of aliphatic amines are based on either direct or indirect oxidation of amine group by observing Faraday current generated, namely by stripping electrons off amine nitrogen atom to its higher oxidation state. The term "direct" or "indirect" is used to describe oxidation processes in which electrons of an analyte are either directly stripped off by the electrode in contact, or by a high oxidation state intermediate or "mediator" which is usually a reversible redox couple having fast kinetics on the electrode.

Many published papers were devoted to indirect electrochemical detection of aliphatic amines and amino acids in flow system such as flow injection analysis (FIA) and

liquid chromatography (LC). Examples are 1) amperometric detection by pre- or post-column derivatization with electroactive groups [13,14,15,16]; 2) indirect detecting by observing new oxidation waves of analyte and co-exist component [17]; 3) Faraday current observed by reformation of surface metal oxide which is stripped off by amine complexing effect such as that on Cu electrode [18,19]; 4) monitoring signal decreasing of an electrochemically oxidative intermediate caused by amine reduction in reductive amperometric mode [20].

Attempts were also made in searching for direct electrochemical detection scheme but successful one is hardly to see. Carbon paste electrodes implanted with metal oxides [21], catalytic components [22] and enzyme [23] have been used in fabricating amperometric electrode for many years but, due to physical and mechanical instability in flow electrolyte systems, the electrodes are seldom mounted in a commercial instrument. There is also a report on modified conductive polymers for sensing aliphatic amines [24], the characterization of such electrode is generally a tedious work. Anodized Ni electrode has been used for amperometric detection of several amino acids in alkaline solution. It has been reported that nickel oxide was observed in electrolyte which may due to severe electrode corrosion [25]. Cu electrodes are used at moderate potentials for indirect detection of amino acids for more than a decade [26] but lately it has been found that the same electrode can been used for direct detection of amino acids under relatively high potentials at passivated Cu oxides surface [27].

Common electrode materials such as Au, Pt and C do not provide catalytic activity for continuous oxidation of aliphatic amines at electrode surface under constantly applied

potentials. On Au and Pt electrodes, aliphatic amines are tend to adsorb extensively on electrode surface at moderate potentials but desorb at higher potentials because of anodic formation of surface oxides (AuO or PtO) as voltammogram indicated. The surface oxides are not electrocatalytic active indeed to support further oxidation of amines in a continuous fashion, therefore Faraday current has been greatly attenuated and even shut down at oxide formation potentials. A genius way to solve this dilemma is by quickly switch applied potentials to large negative values subsequently to achieve cathodic dissolution of the oxides and restore the native reactivity of the clean surface. By using modern personal computer and robust techniques, fast switch of analog potentials and simultaneous acquisition of current signals in millisecond time range are technically possible. The technique is termed as "pulse amperometric detection" (PAD) or more general "pulsed electrochemical detection" (PED) and has been successfully applied in ion chromatography (IC) detection of optically inert polar organics such as carbohydrates, amino acids and thiols [28].

Anodic Oxidation of Aliphatic Amines

Amperometric detection is based on observation of Faraday signals through gain or loss of electrons from or to analyte by redox reactions. In aqueous solution the maximum redox current of a solid electrode can acquire is limited by diffusional rate of analyte from solution to electrode surface, suppose that any pre- or post-chemical reaction rate is infinitely large. This maximum current is also a function of electrode area, number of electron transfered per mole of analyte, concentration and diffusional coefficient of

analyte, and viscosity coefficient of electrolyte. The standard oxidation potential (E^0) of an analyte is a thermodynamic parameter which is virtually different one from another depending on chemical structure of the analyte and electrolyte conditions such as pH and ionic strength. But half wave potential ($E_{1/2}$) of a redox reaction is a kinetic term which depends on heterogenous electron transfer rate, kinetic reaction rate, catalytic effects, and electrode material, structure and morphology. In a narrow potential window of redox reactions in aqueous solution confined by oxygen and hydrogen evolutions, successful observation of distinct current signal through oxidation depends not only on reaction thermodynamics but also on kinetic factors. It can be safely saying that the progress of electrochemistry relies in some way on the development of electrode materials.

Most of the past efforts in investigating new anode materials for the anodic oxidation of aliphatic amines were focused on discovering new electroorganic synthetic pathways. The electrodes used for such purpose are Pt [29,30,31], PbO_2 [32], glassy carbon [33,34], metal Ag [35,36,37], Cu [35, 38,39,40], Ni [35,41,42], Co [35] and even spinel $NiCo_2O_4$ [43].

Platinum and PbO_2 electrodes have long been used for anodic oxidation of aliphatic amines and amino acids in non-aqueous solutions such as acetonitrile and dimethyl sulfoxide (DMSO) and the main products determined were aldehydes in general [31]. At least two waveforms were observed at glassy carbon electrode in alkaline solutions at positive potential regions by cycle voltammetry. Constant potential electrolysis at the electrode indicated that decarboxylation, *ie.*, the loss of carbon dioxide had occurred with aldehydes formation as main product [34]. Oxidation of aliphatic

primary and secondary amines in alkaline were also studied at Ag electrode and found that reaction rate was fast at potential above the AgO formation for primary amines [36] but slow for secondary amines [37]. Nickel electrode placed in contact with alkaline solution has shown to be covered by a layer of nickel hydroxide. At elevated potentials a higher oxidation state nickel oxide (NiO(OH)) was formed which was responsible for the oxidation of organics such as aliphatic amines [41]. In fact a comprehensive study of the oxidation of aliphatic amines at Cu, Co, Ag and Ni electrodes indicated that the reaction happened at potentials where higher oxides were formed such as Cu(II)→Cu(III), Co(II)→Co(III), Ag(I)→Ag(II) and Ni(II)→Ni(III) [35].

Among these electrodes showing catalytic activity, only Ni and Cu had ever been tested for amperometric detection of aliphatic amines or amino acids. No report was found for using other metal electrodes in amperometric detection purpose. This is either because the anticipated electron transfer rate is too slow or because anodizely formed metal oxide is not tightly bound to electrode surface enough to prevent striping loss of metallic sites by amine complexation corrosion.

Mechanism of Oxygen Transfer Reaction-The Role of Oxygen Evolution

The mechanism and kinetic pathways of oxygen evolution at metals and metallic oxide electrodes have long been studied [44,45,46,47]. It is generally believed that the initial step in oxygen evolution involves discharge of water at oxide covered surface to produce adsorbed hydroxyl radicals ($\bullet OH_{ads}$) as following equation indicated:

$$H_2O \rightarrow \bullet OH_{ads} + H^+ + e^- \quad (2)$$

The adsorbed hydroxyl radicals in turn combined with oxygen atoms presented in surface oxide to form dioxygen which is evidenced by a study of isotope oxygen-18 labeled oxide electrode evolving half oxygen-18 labeled dioxygen ^{18}O-^{16}O gas in ^{16}O aqueous solution [48]. By presuming that rate determining step in oxygen evolution involves dissociation of metal-oxygen bonds at the anodes, a linear correlation between overpotential of oxygen evolution and metal-oxygen bond energy has been made [45]. The concept that surface oxygen removal involves inner oxide phase change has been a test of linear plot of overpotential (η_{O2}) with enthalpy of transition between the two highest oxides of many anode materials [49]. Detailed oxygen evolution pathways following surface radical formation and regeneration of surface active site have been proposed by many researches in different situations and are subject to latter modifications [50,51,52].

Anodic oxidation of oxidative species evolving water discharge and oxygen evolution is a general phenomena of any anodic process in aqueous solution. But how water discharge will incorporate in the oxidation steps kinetically and catalytically is still unknown and of great theoretical and experimental importance. The first perceptive correlation of co-production of O_2 which might catalyze other anodic O-transfer reactions was made by In-Hyeong Yeo and co-workers in studying electrocatalytic oxidation of DMSO by bismuth-doped lead dioxide [53]. Joseph E. Vitt and Dennis C. Johnson systematically studied anodic oxidation of I^- to I_2 or IO_3^- at different anode materials by

correlation halfwave potential ($E_{1/2}$) with oxygen evolution overpotential (η_{O2}) and concluded that the anodic discharge of water is a prerequisite of these anodic O-transfer mechanisms [54]. Based on this concept many new anodic materials have been found which shown significant electrocatalytic activity for oxidation of those electrochemically once inert compounds such as sulfite, thiosulfate and dithionite [55], cyanide [56,57,58], thiophene derivatives [59], aliphatic amines [60] and ammonia [61]. These successful examples clearly prove that in-depth understanding of anodic oxidation mechanism in terms of kinetic, catalytic, solid-liquid interface, surface oxide structure, composition and morphology really benefit scientific activities in searching new electrocatalytic anodes and oxidation schemes which may have significance industrial applications.

ELECTROCATALYSIS OF ANODIC OXYGEN-TRANSFER REACTIONS: ALIPHATIC AMINES AT MIXED SILVER-LEAD OXIDE-FILM ELECTRODES

A paper published in the Journal of Electrochemical Society [1]

Jisheng Ge [2] and Dennis C. Johnson [2,3]

Abstract

Results are described from research directed to the discovery of new anode materials suitable for obtaining stable and sensitive response when applied at constant potential for the amperometric detection of organic amines. Voltammetric and amperometric results are compared for detection of selected organic amines in carbonate buffer (pH 10) at mixed silver-lead oxide films prepared by electrodeposition on platinum substrates and by anodization of Ag-Pb alloys. Anodic response is observed at both electrodes for ethylamine, N-ethylmethylamine, trimethylamine, ethanolamine, and *L*-alanine. However, data indicate the oxide electrode formed by anodization of Ag-Pb alloys is superior with regard to stability of response. On the basis of flow-injection detection using constant applied potential in carbonate buffer, linear dynamic ranges ($r^2 >$ 0.99) are at least three decades for selected primary, secondary, tertiary, alkanolamine, and amino acids in carbonate buffer (pH 10), with detection limits (S/N = 3) of *ca.* 0.3 μM

---

[1] See J. Electrochem. Soc., 1995, 142(5), 1525.

[2] Graduate student and Professor, respectively. Department of Chemistry and Ames Laboratory, Iowa State University, Ames, IA 50010.

[3] Author for correspondence.

(*i.e.*, 6 pmol per 20-μL injection). Results also are presented for the characterization of these films using x-ray diffractometry, x-ray photoelectron spectroscopy, and scanning electron microscopy.

Introduction

The widespread existence of organic amines in biological systems and pharmaceutical formulations represents a challenge to analytical chemists. The low volatility of the majority of these compounds tends to preclude their direct quantitative determination by gas chromatography (GC). Furthermore, the general absence of strong chromophoric and/or fluorophoric functional groups has hindered their direct detection by conventional photometric techniques without *a priori* derivatization.

Direct electroanalytical detection of aliphatic amines is conceivable only on the basis of anodic reactions; however, successful electrochemical oxidation of these compounds has appeared elusive [1]. This probably results because the corresponding reactions necessitate transfer of oxygen from H_2O in the solvent phase to the oxidation product(s) and conventional anode materials (*e.g.*, Pt, Au, and C) apparently lack the ability to support these O-transfer mechanisms, when operated at constant applied potentials, without interference from large background currents from anodic discharge of H_2O to produce O_2. Recent developments in the application of pulsed-potential waveforms applied at gold electrodes have been highly successful for so-called *pulsed electrochemical detection* (PED) of organic amines with detection limits at the picomolar

level when applied in liquid chromatographic systems [2]. The success of PED is the result of electrocatalytic mechanisms believed to involve the anodic discharge of H_2O with generation of transient adsorbed hydroxyl radicals ($\cdot OH_{ads}$) as an intermediate product in the formation of inert surface oxide (AuO). Hence, the catalytically-active state of the gold surface is short lived (< *ca.* 1 s) and "continuous" detection in liquid chromatography (LC) systems is accomplished only by multi-step potential-time waveforms which alternate the processes of electrocatalytic detection with subsequent cathodic reduction of surface oxide prior to repetition of the detection cycle.

Our desire to achieve a significant improvement in detection limits for aliphatic amines and amino acids separated by liquid chromatography has stimulated a search for new anode materials that retain their catalytic activity indefinitely when operated at constant potential. These are expected to have significantly improved signal:noise response as compared to PED because of greater ease in discrimination against noise in constant-potential amperometry. Characteristics anticipated for these new catalytic anodes include: (i) use of metal oxides with minimal solubility in aqueous phases under the pH conditions of application, (ii) existence of a low density of surface sites at which the anodic discharge of H_2O with evolution of O_2 occurs at a significantly lower overpotential than is characteristic of the majority surface matrix, and (iii) existence of surface sites that are effective for adsorption of the non-bonded electron pair of the N-atoms in amine compounds. Adsorption is believed to be important because of a suspected need to desolvate the electronic orbital to which oxygen from adsorbed $\cdot OH$ is to be transferred, *i.e.*, oxygen transfer cannot occur by a tunneling mechanism. The choice of electrode

composition tested in this research follows from the work of Yeo *et al.* who doped β-PbO_2 film electrodes with Bi(V) and observed significant activation for several O-transfer reactions [3] with simultaneous but small decreases in net O_2-evolution overpotential [4]. The choice of silver as the cationic dopant follows from the common knowledge that Ag(I) forms stable coordination bonds with amines in their aqueous solutions. Some reports have appeared describing slow anodic oxidation of organic amines at anodized silver electrodes in alkaline media for the purpose of electroorganic syntheses [5]; however, these reports do not indicate the existence of a transport-limited response that is a prerequisite for reliable electroanalytical applications of these electrode materials.

Significant reports have appeared regarding anodic detection of a variety of organic compounds at non-noble metal oxide electrodes under constant applied potentials. Anodized nickel electrodes have been applied for detection of alcohols, amines, thiols, and carbohydrates [6,7]. Anodic response has been proposed to involve a surface-mediated mechanisms involving Ni(III) formed in the oxide film at large positive potentials [8]. A disadvantage of using the anodized nickel electrodes is the apparent need for addition of $(NiOH^+)_4$ to the solution phase to minimize dissolution of the slightly soluble metal oxide [9]. The mediated oxidations are under kinetic control and, therefore, anodic response exhibits high sensitivity to temperature fluctuations and elevated temperature is recommended for maximizing anodic response [10]. The dynamic range for amines and amino acids determined in a flow-injection system was reported to be approximately three decades with a detection limit for glycine of a few nanograms [7]. Indirect anodic detection of amino acids has been described at anodized copper electrodes [11,12]. The

response mechanism is proposed to correspond to dissolution of copper(II) oxide or hydroxide layer as a result of chelation of Cu(II) by the amino acids followed by anodic reformation of passive oxide film [12]. Hence, the response time is limited by the rate determining step of dissolution which results in a strong dependence of the signal on the eluent flow rate in liquid chromatographic applications [13]. The long-term stability of these electrodes is suspect, because of the nature of the response mechanism, and this has apparently restricted widespread acceptance of this electrode. Luo *et al.* have described results of a voltammetric study of amino acid response at copper electrodes in alkaline media [14]. They confirmed that the indirect detection occurs at low positive potentials; however, they discovered that the amino acids are detected by a direct anodic process at high positive potentials. Using the direct anodic mechanism for detection of amino acids in a flow-injection system, they determined that detection limits for some amino acids are at the sub-nanogram level [14]. We find no reports indicating that researchers have examined the response for aliphatic amines at doped and/or mixed-metal oxide electrodes.

Experimental

Chemicals

Chemicals were analytical grade (Fisher Scientific, Sigma, and Eastman Kodak) and were used as received. Water was distilled and purified further in a NANOpure II system (SYBRON/Barnstead). Supporting electrolytes included 0.10 M $HClO_4$, 0.10 M NaOH, 0.10 M NaH_2PO_3-Na_2HPO_3 (pH 7.0), 0.10 M $NaHCO_3$-Na_2CO_3 (pH 10), 0.025 M

$Na_2B_4O_7$ (pH 11), and 0.10 M Na_2HPO_3-Na_3PO_3 (pH 12). Stock solutions of Pb(II) and Ag(I) solutions were prepared from $Pb(NO_3)_2$ and $AgNO_3$, respectively. Concentrations of stock solutions of aliphatic amines were determined by acidimetric titration following dissolution of the commercial reagents in purified water [15].

Electrode preparation

The Pt rotated disk electrode (RDE, 0.46 cm^2; Pine Instrument Co.) was polished with 0.05-μm alumina on microcloth (Buehler Ltd.) prior to each film deposition. Lead oxide films were electrodeposited from 0.1 M $HClO_4$ (1.5 V, 30 min, 400 rev min^{-1}) and from 0.1 M carbonate buffer (0.9 V, 30 min, 1600 rev min^{-1}) each containing 0.2 mM Pb(II). Silver oxide films and mixed Ag-Pb oxide films also were electrodeposited from 0.1 M carbonate buffer (1.0 V, 30 min, 400 rev min^{-1}) containing specified concentrations of Ag(I) and Pb(II).

Additional metal oxide and mixed-metal oxide-film electrodes where prepared by anodization of Ag, Pb and Ag-Pb alloys prepared in the form of rotated disks (*ca.* 0.20 cm^2). Alloys corresponded to Ag:Pb ratios (wt.:wt.) of 1:5 and 1:20 containing 16.7% and 4.8% Ag by weight, respectively; and the eutectic phase which contains 2.4% Ag by weight. These alloys were fabricated in-house from metals prepared by melting the appropriate pure metal powders in evacuated quartz tubes over a Meeker burner with constant shaking (*ca.* 30 min). After cooling, the tubes were broken and the metals retrieved. Rods of these metals (0.50-cm dia. X 1.0-cm length) were produced using a hydraulic laboratory press (Fred S. Carver, Inc.) at a pressure of 3,000 to 4,000 lbs in^{-2}.

The end surface of each rod was machined perpendicular to its axis, inserted into a Teflon cylinder, and sealed by wax to prevent flow of solution between the metal and the inner surface of the Teflon. Excess wax was removed from the end of the assembly. One end of the rod surrounded by Teflon was connected to the end of a stainless steel rod previously machined for attachment to an ASR rotator (Pine Instrument Co.). The other end of the rod was prepared for use as a RDE by grinding with sand paper (P1200, SIA, Swiss) followed by anodization in carbonate buffer (0.9 V, 5 min, 400 rev min^{-1}) to produce a layer of surface oxide.

Instrumentation

Voltammetric data were obtained using a model RDE3 potentiostat and model ASR rotator (Pine Instrument Co.) under control by a desktop computer (IBM) equipped with a DT2801 interface (Data Translation) and ASYST-3.1 software (Keithley/Asyst). The counter electrode was a Pt wire and the reference electrode was a saturated calomel electrode (SCE, Fisher Scientific). All potentials are reported *vs.* the SCE. Voltammetry at electrodeposited film electrodes was restricted to the limits 0.7 V and 1.1 V (pH 10) to prevent cathodic reduction of the films and excessive anodic evolution of O_2, respectively.

One flow-injection detection (FID) system consisted of a digitally controlled peristaltic model EVA pump module and EVA valve module (Eppendorf North America, Inc.) with 50-μL sample loop. A second FID system was assembled from a dual-piston hydraulic model AMPL-1 pump (Dionex Corp.) and a model 7010 injection valve (Rheodyne) with a 20-μL sample loop. The flow-through detector was constructed

according to a published design [16] with electrodes made from wires (*ca.* 1 mm dia.) of anodized Ag-Pb alloy mounted in a wall-jet configuration. Analog recording of FID data utilized a D5216-1BA stripchart recorder (Bausch and Lomb). Digital recording utilized a subroutine prepared in ASYST 3.1 software with programmable acquisition rate (*e.g.*, an acquisition rate of 1.25 Hz produced *ca.* 40 data points per FID peak).

X-ray diffractometry (XRD) was performed using a XDS-2000 (Scintag) diffractometer with a Peltier detector (Devex) based on source. The 2θ (two-theta) angle of the diffractometer was stepped from 10 to 70° by 0.03° increments. X-ray photoelectron spectroscopy (XPS) was performed using a PHI 5500 spectrometer (MutiTechnique) equipped with a monochromatic Al-Kα source. Surface imaging and elemental mapping were performed using a S-2460N (Hitachi) scanning electron microscope (SEM) and data were analyzed using a Link ISIS microanalysis system (Oxford Instruments). Some samples were electrodeposited onto gold films that had been vapor deposited on quartz plates [17] and then platinized in 0.2 M H_2SO_4 containing 2 mM H_2PtCl_6 [18]. Other samples were prepared by anodization of Ag-Pb alloy blocks.

Product identification was achieved by gas chromatography with mass spectrometry, using a model 4000 GC-MS (Finnigan), applied to the diethylether extracts.

Results and Discussion

Preliminary results

Lead oxide films deposited from both acidic and alkaline media showed no significant activity for ethylamine in carbonate buffer. Likewise, electrodeposited silver oxide films exhibited no significant activity for ethylamine. Furthermore, the silver oxide films were easily removed from the Pt substrate by wiping with a soft tissue and also were observed to dissolve during prolonged exposure to high ethylamine concentrations (> 10 mM) in the carbonate buffer, probably by a chemical stripping mechanism.

Large anodic and cathodic residual currents were obtained for an anodized Ag electrode in carbonate buffer within a potential range defined by the limits for anodic and cathodic discharge of H_2O with evolution of O_2 and H_2, respectively. These residual currents were concluded to correspond to anodic formation (pos. scan) and cathodic dissolution (neg. scan) of surface oxide on the Ag substrate. The residual currents (pos. scan) for cyclic scans within the limits 0.7 and 1.1 V were observed to decrease by a factor of *ca.* 50X with addition of ethylamine; however, no significant anodic response was observed for ethylamine. This observation is interpreted to be an indication that ethylamine is strongly adsorbed at the anodized Ag surface. Furthermore, this evidence for adsorption supports the premise that silver oxide sites in mixed silver-lead oxide electrodes can function as adsorption sites for organic amines within the desired anodic O-transfer reaction mechanisms.

Electrodeposited Ag-Pb oxide films

In sharp contrast to the above results, well defined anodic waves are obtained for ethylamine using electrodeposited silver-lead oxide electrodes in carbonate buffer (pH 10). Typical voltammetric curves (i-E) are represented in Figure 1.1 for 3.9 mM ethylamine (solid lines) in comparison to the residual response (dashed lines) as a function of the ratio [Ag(I)]/[Pb(II)] in the deposition solutions. The curves shown were obtained during the positive scan; however, during the negative scan, these curves were retraced except for slight differences attributable to charging currents. It is evident in Figure 1 that the presumed increase in the Ag:Pb ratio in the electrodeposited films, resulting from increased values of the ratio [Ag(I)]/Pb(II)] in the deposition solution, results in a significant increase in residual current for H_2O, discharge with O_2 evolution, with the accompanying benefit of increased anodic response for ethylamine. These observations support the initial premise that electrocatalytic oxidation of aliphatic amines requires incorporation of surface sites (silver oxide) characterized by O_2-evolution overpotentials that are smaller than that for the host matrix (lead oxide). A similar correlation between anodic O-transfer reactivity and decreased net overpotential for O_2 evolution has been observed for Bi(V)-doped β-PbO_2 films electrodes [4]. These results are in agreement with the conclusion that the rate-controlling step in anodic O-transfer reaction is the discharge of H_2O [19].

Visual inspection of the data in Figure 1.1 reveals that net voltammetric response for ethylamine, i.e., total response minus the residual response, is peak shaped for all film compositions. As a result of the peaked response, the net current for ethylamine at E »

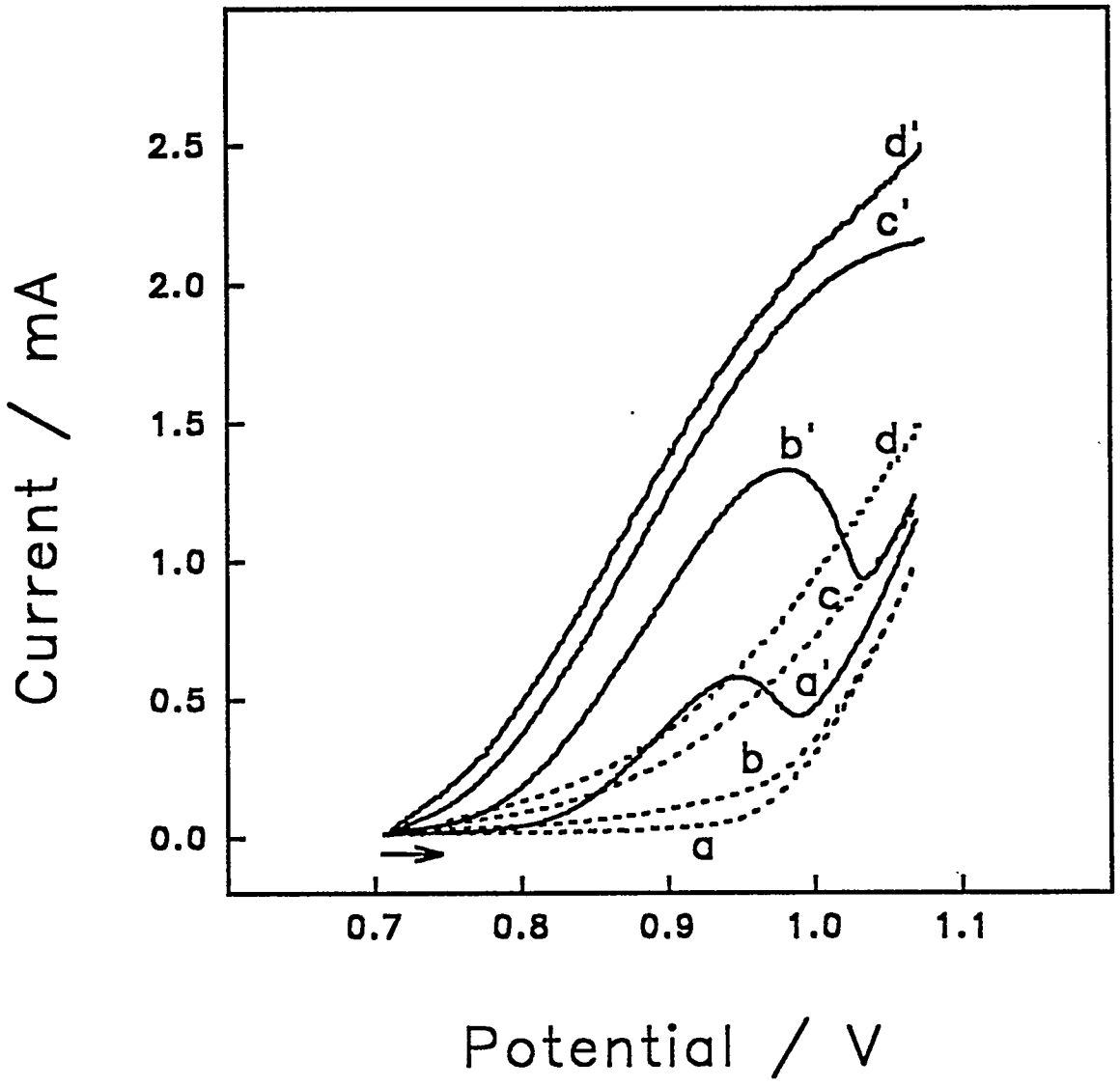

Figure 1.1. Voltammetric response (pos. scan) for ethylamine at various electrodeposited Ag-Pb oxide rotated disk electrodes in carbonate buffer (pH 10). Scan rate: 2.0 V min^{-1}. Rotation speed: 3600 rev min^{-1}. Film-deposition solution: 40 μM Pb(II) with variable Ag(I) in carbonate buffer (pH 10); [Ag(I)]/[Pb(II)]: (a,a') 1/40, (b,b') 1/10, (c,c') 1/4, (d,d') 1/2. Ethylamine concentration (mM): (- - - -) 0, (———) 3.9.

1.0 V is only slightly larger than the residual current resulting from anodic discharge of H_2O with evolution of O_2. Upon scan reversal at 1.1 V, the peak-shaped response is retraced, except for small differences attributable to charging currents. Therefore, it is apparent that the peaked response for the amine is not the result of some irreversible fouling of the electrode surface caused by adsorption of ethylamine and/or its oxidation product(s). We speculate that silver sites in the surface of the mixed silver-lead oxide electrode can function to adsorb both the amine group of ethylamine and the hydroxyl radicals (·OH) generated as the intermediate product in the O_2 evolution reaction. Accordingly, as the rate of ·OH generation increases with increasing potential, the adsorbed ·OH interferes with adsorption of ethylamine and, as a consequence, the desired O-transfer mechanism is blocked for ethylamine oxidation.

A systematic study revealed that the Ag-Pb oxide films deposited from carbonate buffer containing [Ag(I)]:[Pb(II)] = *ca.* 0.15 produced the largest background-corrected peak response for ethylamine. For [Ag(I)]:[Pb(II)] increasing beyond 0.15, the net peak response decreased. Recall from above that virtually no useful anodic response is observed for a pure Ag-oxide film electrodeposited from carbonate buffer.

Electrodeposited Ag-Pb oxide films on the Pt RDE were shiny in appearance with a dark reddish-orange coloration. These films were adherent and not easily removed by rubbing with absorbent tissues. Voltammetric and amperometric response for ethylamine at these electrodeposited film electrodes were not stable for high amine concentrations. For example, the chronoamperometric response obtained for 50 mM ethylamine at 0.95 V decayed continuously over a 30-min period. Prolonged exposure of the electrodeposited

Ag-Pb oxide films to ethylamine (0.95 V) resulted ultimately in complete dissolution of the films.

The tedious preparation procedures and poor stability of the electrodeposited Ag-Pb oxide films observed at high amine concentrations mitigates against their use in the analytical laboratory. Whereas results obtained for ethylamine indicate this mixed oxide has potential for anodic detection of organic amines, alternate means of preparation are required to achieve greater film stability.

Anodized Ag-Pb alloys

The partial success obtained for electrodeposited Ag-Pb oxide films led to examination of the activity of anodized Ag-Pb alloys for anodic detection of aliphatic amines. Anodized Ag-Pb alloy electrodes are easily prepared and offer the potential advantage of a virtually infinite resource of material for reformation of surface oxides in the event of slow dissolution of these films. Shown in Figure 1.2 is the voltammetric response (pos. scan) obtained at the anodized eutectic phase Ag-Pb alloy RDE in carbonate buffer as a function of added ethylamine. It is apparent that the net response (background corrected) is peak shaped, as was observed at the electrodeposited Ag-Pb oxide films (Figure 1.1). Hence, the voltammetric response indicates that the response mechanism is the same for the electrodeposited and anodized Ag-Pb oxide surfaces. Shown in Figure 1.3 is the voltammetric response (pos. scan) for 2.0 mM ethylamine in carbonate buffer obtained as a function of rotation speed at an anodized eutectic-phase Ag-Pb alloy. A plot (not shown) of the reciprocal peak response ($1/i_{peak}$) at 0.95 V *vs.* the

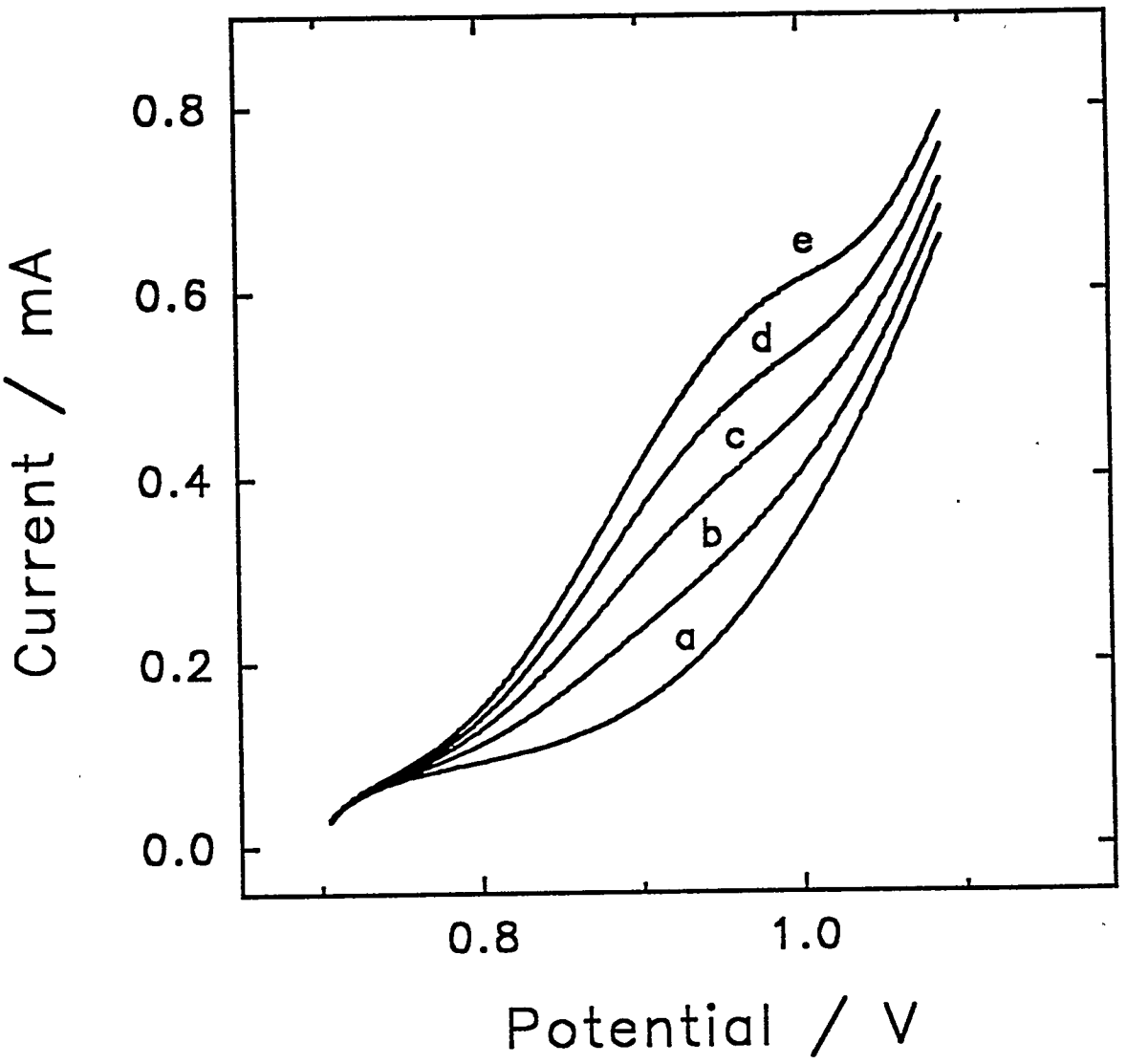

Figure 1.2. Voltammetric response (pos. scan) at an anodized eutectic-phase Ag-Pb alloy RDE as a function of ethylamine concentration in carbonate buffer (pH 10). Scan rate: 2.0 V min^{-1}. Rotation speed: 1600 rev min^{-1}. Ethylamine concentration (mM): (a) 0, (b) 0.5, (c) 1.0, (d) 1.5, (e) 2.0.

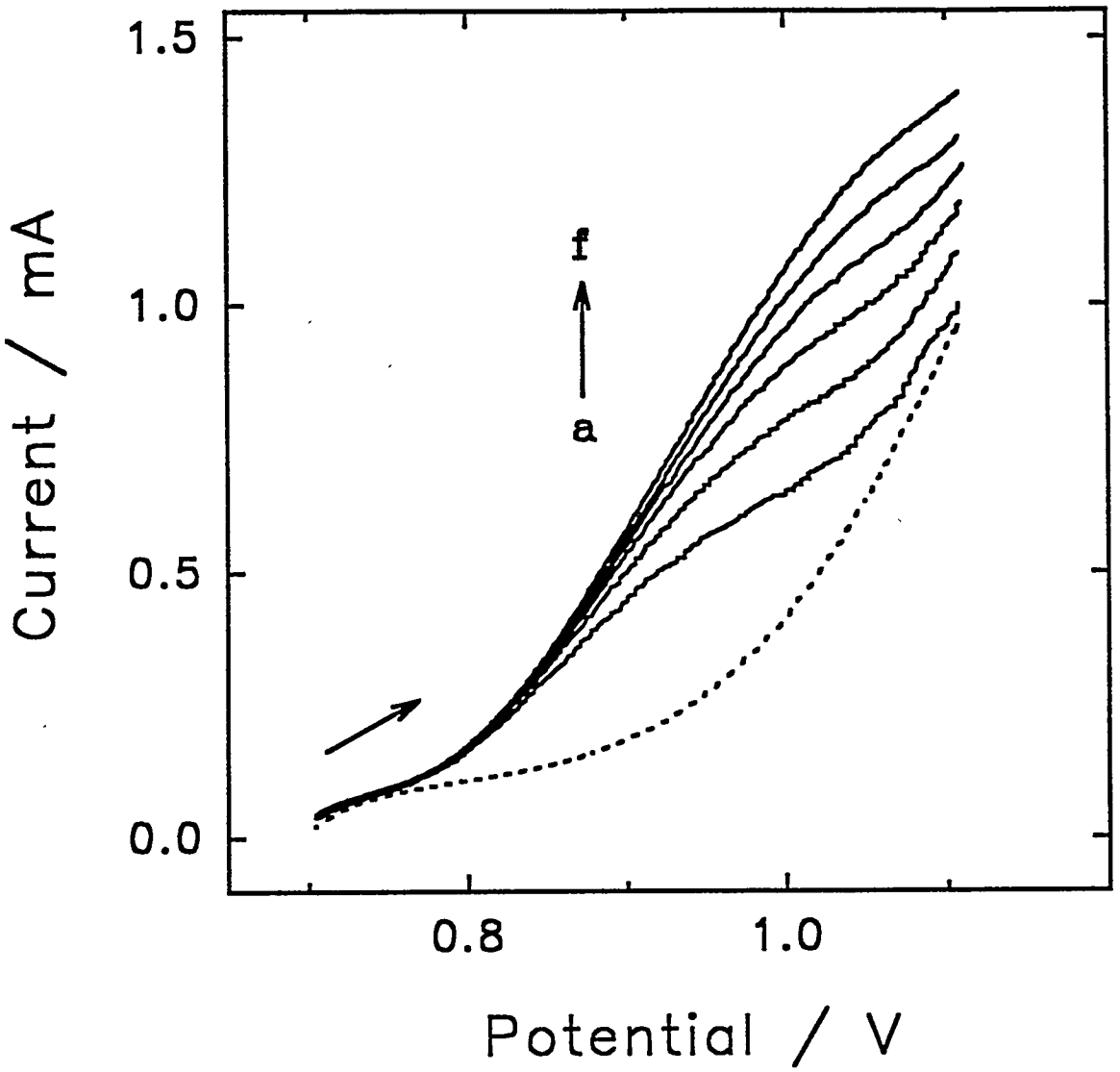

Figure 1.3. Voltammetric response (pos. scan) for ethylamine at an anodized eutectic-phase Ag-Pb alloy RDE as a function of rotation speed in 0.1 M carbonate buffer (pH 10). Scan rate: 2.0 V min^{-1}. Ethylamine concentration (mM): (- - - -) 0, (———) 2.0. Rotation speed (rev min^{-1}): (a) 400, (b) 900, (c) 1600, (d) 2500, (e) 3600, (f) 4900.

reciprocal square root of rotation speed ($1/\omega^{1/2}$), commonly known as the Koutecky-Levich plot [20], was linear with a non-zero intercept. This is evidence for an electrode process under mixed control by the rates of mass transport and heterogeneous kinetics. The voltammetric response was examined also for a variety of organic amines. Included were butylamine, N-ethylmethylamine and trimethylamine, as examples of primary, secondary and tertiary amines, respectively; and ethanolamine and L-alanine as examples of alkanolamines and amino acids, respectively. These *i-E* curves were very similar to that for ethylamine without significant differences in peak potential. Furthermore, as observed for ethylamine, plots of $1/i_{peak}$ *vs.* $1/\omega^{1/2}$ for each compound were linear with non-zero intercepts, as evidence of mixed transport-kinetic control. Based on the similarities between these data, the response mechanisms for these aliphatic amines are considered to the virtually identical without significant effects from adjacent functional groups. No response was observed for ethanol, ethylaldehyde, acetone, glucose, and acetonitrile. The chronoamperometric response (0.95 V) for 2.0 mM ethylamine at a newly anodized eutectic-phase Ag-Pb alloy electrode quickly reached a stable value within *ca.* 4 min. Also, there was no evidence for loss of sensitivity over an extended time period (30 min). Hence, it is apparent that the anodized Ag-Pb alloy electrode is not fouled during oxidation of ethylamine. Voltammetric response for ethylamine also was examined in various supporting electrolyte to determine the effects of changing pH and the corresponding anionic species. The peak current response in borax buffer (pH 11) and phosphate buffer (pH 12) were virtually identical to that for carbonate buffer (pH 10), with only slight differences in peak potential. However, no amine response was observed

in the neutral phosphate buffer (pH 7). This observation is explained on the basis of protonation of the amine group at pH « 10 which, in turn, prevents adsorption at the Ag-Pb oxide surface.

It was determined that addition of Cl^- to the carbonate buffer produced significant attenuation of the amine response at all Ag-Pb oxide electrodes. Shown in Figure 1.4 (solid lines) are representative *i-E* curves for 2.0 mM ethylamine as a function of added Cl^- obtained at the anodized eutectic-phase Ag-Pb alloy electrode. The effect of Cl^- on the residual response (dashed lines) also is shown for comparison. Clearly, added Cl^- produces a decrease in the net rate of H_2O discharge as well as the anodic response for ethylamine. We surmise without proof that Cl^- is strongly adsorbed at the silver sites in the mixed-oxide surface. Adsorbed Cl^- at silver sites can interfere with the response mechanism by blocking the discharge of H_2O well as amine adsorption at these sites. There was no change in the appearance of the surface of the anodized eutectic-phase alloy electrode as a consequence of exposure to 0.1 mM Cl^-. However, the surfaces of anodized alloys with greater Ag content (> 2.4% by wt.) acquired a definite whitish coloration when exposed to 0.1 mM Cl^-. These results are understood on the basis of adsorption of Cl^- only to silver sites in the Ag-Pb oxide surface.

Flow-injection detection

Linear dynamic ranges and detection limits were calculated for ethylamine, N-ethylmethylamine, trimethylamine and L-alanine on the basis of data obtained using the flow injection detection (FID) system. Typical data are shown in Figure 1.5 for

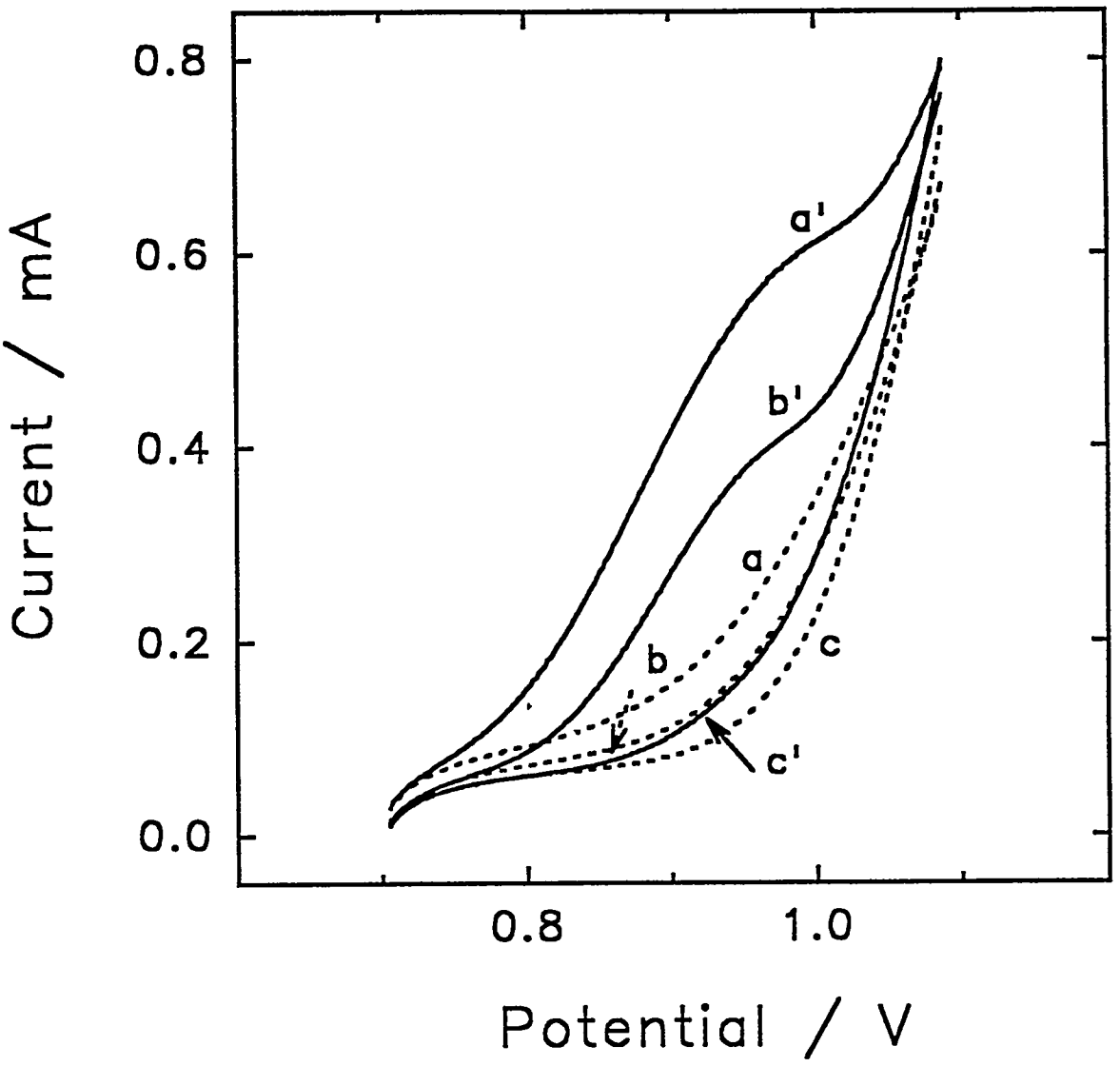

Figure 1.4. Effect of added Cl^- on voltammetric response (pos. scan) for ethylamine at an anodized eutectic-phase Ag-Pb RDE in 0.1 M carbonate buffer (pH 10). Scan rate: 2.0 V min^{-1}. Rotation speed: 1600 rev min^{-1}. Curves: (- - - -) residual, (———) 2.0 ethylamine. Concentration NaCl (mM): (a,a′) 0, (b,b′) 10, (c,c′) 100.

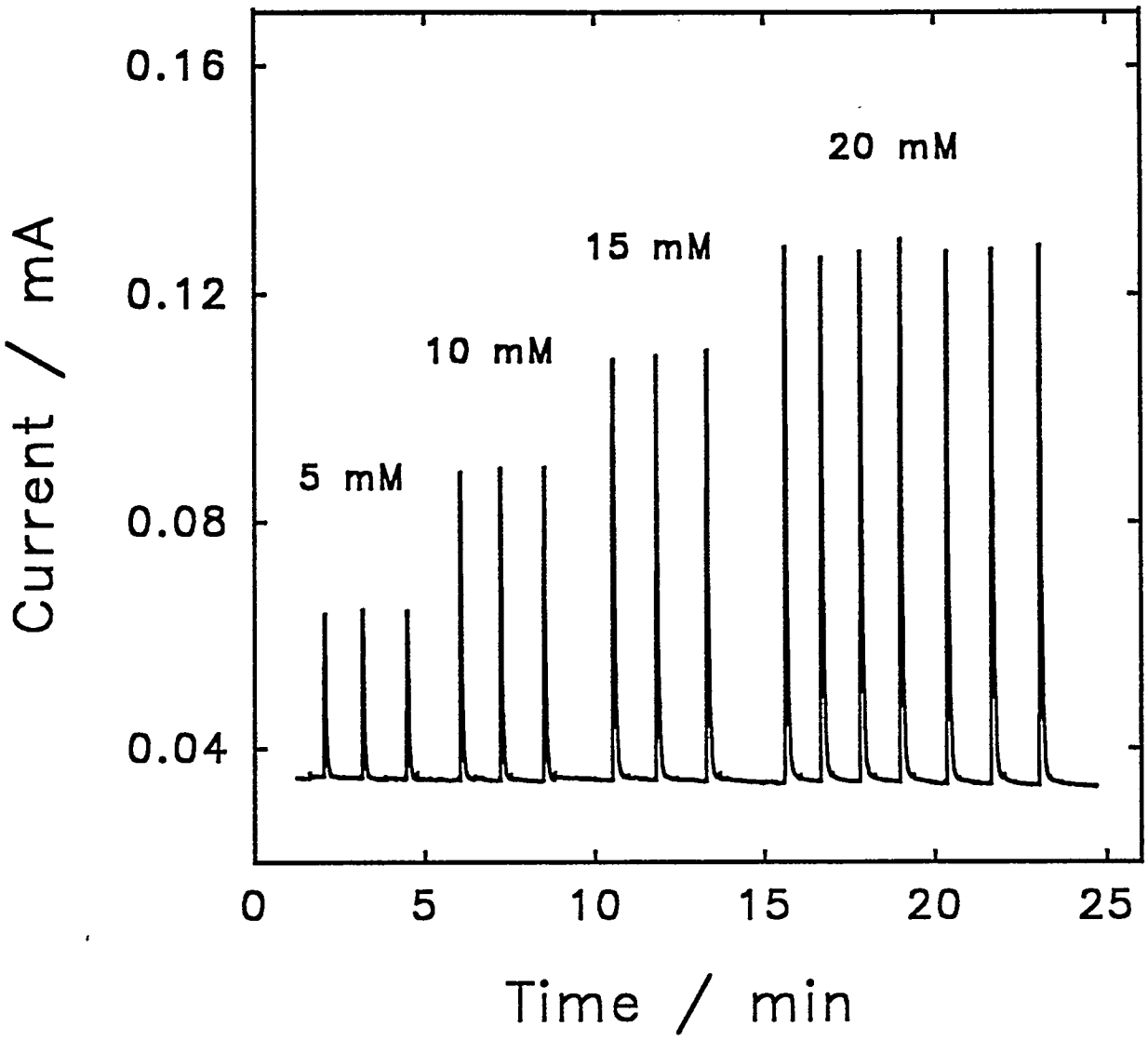

Figure 1.5. Representative flow-injection detection peaks for ethylamine at an anodized eutectic-phase Ag-Pb alloy electrode in 0.1 M carbonate buffer (pH 10). Carrier phase: 0.1 M carbonate buffer, 1.0 mL min^{-1}. Potential: 0.90 V *vs.* SCE. Sample loop: 50 μL. Ethylamine concentrations: given in figure.

ethylamine. The linear dynamic range ($r^2 > 0.99$) was determined to be at least three decades for selected primary, secondary, tertiary, alkanolamine, and amino acids in carbonate buffer (pH 10), with limits of detection (S/N = 3) equal to *ca.* 0.3 μM (*i.e.*, 6pmol per 20-μL injection). Addition of the organic modifiers acetonitrile, acetaldehyde, acetone, and ethanol into the mobile phase did not attenuate the amine signals.

The long-term stability of the anodized eutectic-phase Ag-Pb alloy electrode was determined over a 45-hr period (540 injections of 1.0 mM ethylamine). Relative standard deviations of the peak response were *ca.* 1% for individual 5-hr periods (60 injections) and 4.7% for the total 45-hr period. There was no apparent deterioration of peak signal during the 45-hr period and, furthermore, visual examination of the electrode surface at the conclusion of the test revealed no evidence of corrosion or other physical deterioration of the oxide surface.

In general, a single 30-min period of anodization (0.85 V) applied to new Ag-Pb alloy electrodes mounted in the flow cell, during passage of carbonate buffer, was determined to be sufficient preparation for repeated heavy usage over a several-month period without the need for re-polishing the alloy surface. Thereafter, baselines signals were observed normally to reach steady-state values within a *ca.* 20-min period at the start of each new experimental day.

Reaction products

Solutions of ethylamine and L-alanine in carbonate buffer were exhaustively electrolyzed (0.95 V) at anodized Ag-Pb alloy electrodes. The organic products from

both electrolyses were extracted with diethylether and identified as ethylaldehyde on the basis of GC-MS data. These results are in agreement with reports for other electrodes [21]. Based on this result, we speculate the electrode reaction for aliphatic amines at the anodized Ag-Pb alloy electrode can be represented by:

$$R\text{-}CH_2\text{-}NH_2 + 2OH^- \rightarrow R\text{-}CHO + NH_3 + H_2O + 2e^- \quad (1)$$

and, for amino acids, by:

$$R\text{-}CHNH_2\text{-}COOH + 2OH^- \rightarrow R\text{-}CHO + NH_3 + CO_2 + H_2O + 2e^- \quad (2)$$

These conclusions are supported by the fact that anodic response was not observed for ethylaldehyde to concentrations of 50 mM in carbonate buffer.

Values of *n* based on coulometric data from exhuastive electrolyses were highly variable. Subsequent voltammetric results (not shown) indicate that some anodic response is obtained for NH_3(aq) in carbonate buffer. Hence, we estimate that Equations 2 and 3 represent the primary electrode reactions for amine compounds, and that further oxidation of NH_3 is highly variable at pH 10 due to outgasing under well-stirred conditions. Results from the on-going study of NH_3 oxidation at anodized eutetic-phase Ag-Pb alloy electrode will be the subject of a future report.

X-ray diffractometry (XRD)

Surfaces of Pb become dark red when anodized in carbonate buffer whereas surfaces of the anodized eutectic-phase Ag-Pb alloy turns a reddish-orange color, similar to the color of litharge (PbO). Figure 1.6 contains the XRD spectrum for a 1:5 (wt:wt)

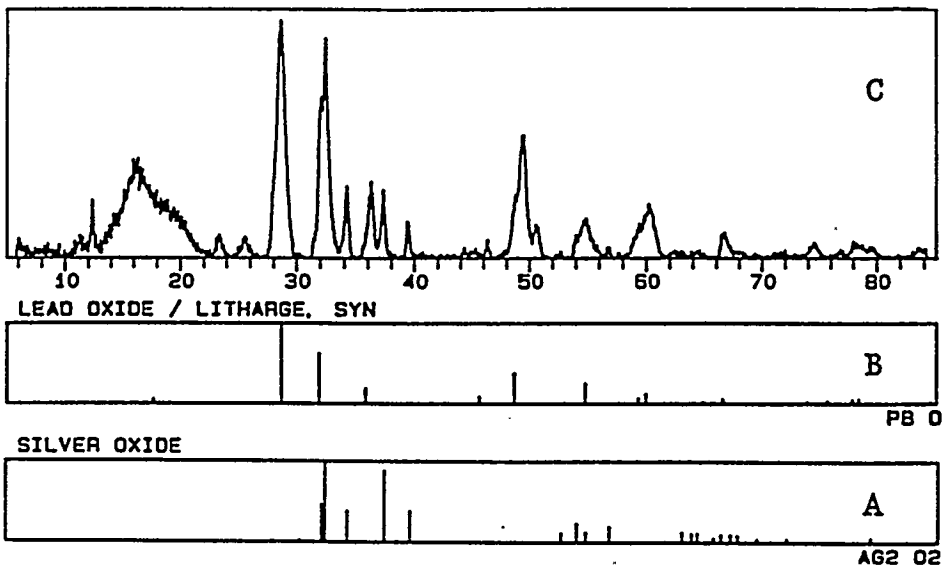

Figure 1.6. X-ray diffraction spectra: (A) silver oxide (AgO); (B) litharge (PbO); and (C) surface of 1:5 (wt:wt) Ag-Pb alloy electrode anodized in 0.1 M carbonate buffer (pH 10) at 0.90 V for 12 hrs.

Ag-Pb alloy (C) anodized in carbonate buffer (0.9 V). Also shown for comparison are standard spectra for AgO (A) and PbO (B) taken from ICPDS files No. 22-0472 and 05-0561, respectively [22]. The strong correspondence between 2θ values for reflections in the standard AgO and PbO spectra with values for the anodized Ag-Pb alloy indicates that the oxide film on the anodized alloy consists primarily of a mixture of AgO and PbO (litharge). There is no indication of a single mixed-metal oxide phase at the surface of anodized Ag-Pb alloys. Minor peaks observed at 2θ = 22 to 26° (Fig. 1.6C) are suspected to correspond to small amounts of PbO_2. However, the roughness of these films causes XRD reflections to be very broad at low 2θ values and they are not reliable for qualitative work.

As expected, the intensity of AgO peaks in XRD spectra for anodized samples of the Ag-Pb alloys decreased with decreasing Ag:Pb ratios. The XRD spectra obtained for the anodized eutectic-phase Ag-Pb alloy (not shown), containing only 2.4% Ag (by wt), contained strong reflections for PbO (litharge) with evidence for a small amount of lead hydroxycarbonate ($Pb_3(CO_3)_2(OH)_2$). No peaks were observed that can be attributed to AgO. Furthermore, no reflections were observed that can be attributed to a mixed Ag-Pb oxide phase. However, it cannot be concluded whether these observation are the result of the absence of these phases or merely the low sensitivity of the XRD technique.

No XRD reflections were obtained for electrodeposited silver-lead oxide films even when data were averaged over a 12-hr acquisition period. These films are believed to be amorphous, *i.e.*, particle sizes less than the wavelength of the Cu-Kα_1 radiation.

X-ray photoelectron spectroscopy (XPS)

The XPS spectrum for the silver region is shown in Figure 1.7 (top) for an anodized 1:20 (wt:wt) Ag-Pb alloy. Slightly conflicting literature values were found for the binding energies in the silver oxides [23,24]. Therefore, reference films were generated in-house by anodization of pure Ag in carbonate buffer at 0.3 V (10 min), to produce a Ag_2O film, and at 0.6 V (10 min), to produce a AgO film [25]. The XPS spectra are included in Figure 1.7 for these AgO (middle) and Ag_2O (bottom) reference films. The binding energies for the Ag $3d_{5/2}$ electrons of the Ag_2O and AgO films are 367.8 ev and 367.5 ev, respectively. These energies are in agreement with one report of 367.9 ev for Ag_2O and 367.5 ev for AgO [24]. The chemical shifts of silver have the abnormal tendency to move to lower energy as oxidation state is increased [26].

The difference in binding energies for Ag_2O and AgO are very small (*ca.* 0.4 ev) and, therefore, it is difficult to specify with great certainty the exact identity of the oxidation state for silver at the surface of the anodized Ag-Pb alloy. However, because the peak positions observed in Figure 1.7 for the anodized Ag-Pb alloy most closely match those for the AgO reference, the silver in the anodized alloy film is concluded to correspond primarily to AgO. We note that both peaks for the anodized alloy have slight shoulders at energies slightly higher than at the peak energy and these shoulders might be indicative of the presence of some Ag_2O. The poor resolution of the spectrometer (*ca.* 0.5 ev @ 5.85 ev) discouraged us from attempts at estimation of relative amounts of Ag_2O and AgO in the oxide films on anodized Ag-Pb alloys.

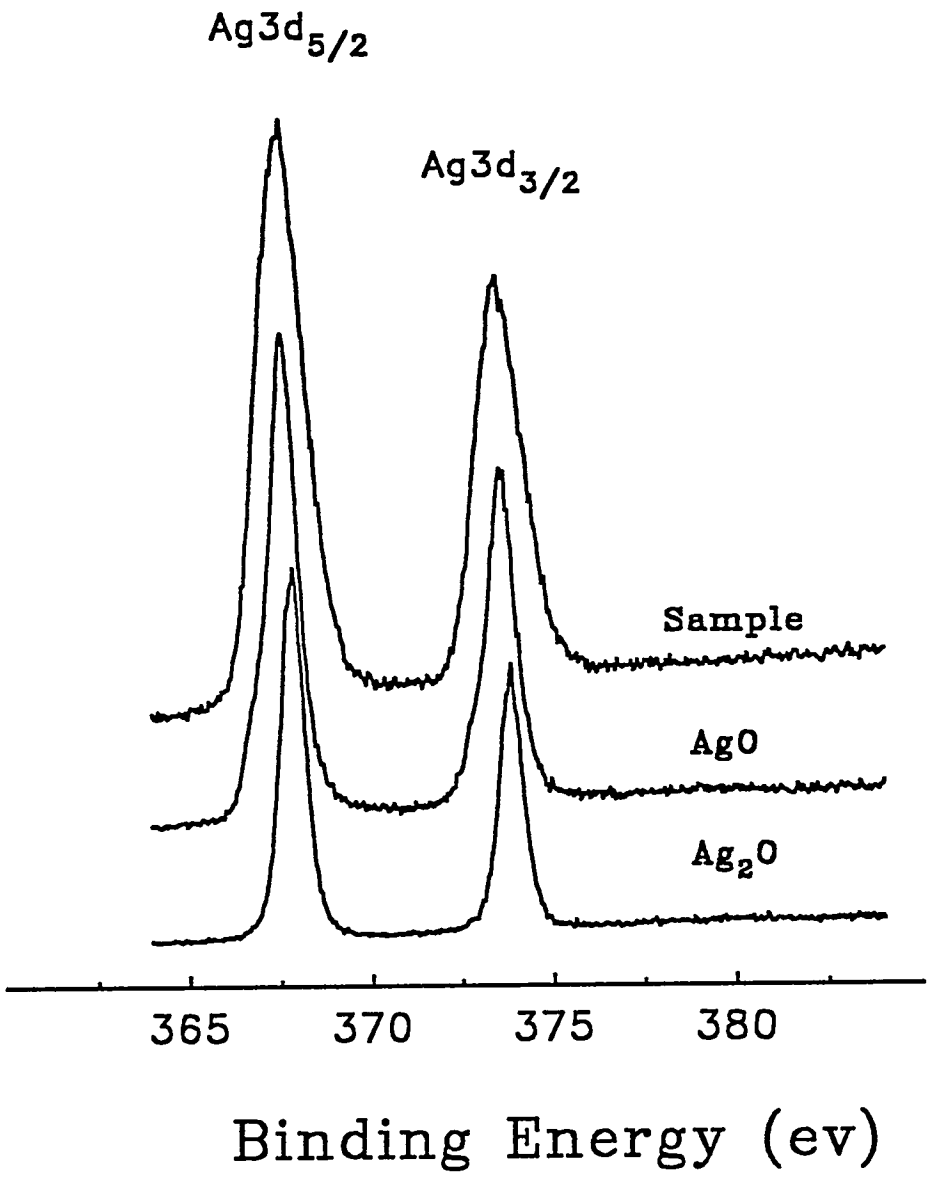

Figure 1.7. X-ray photon spectra showing Ag $3d_{5/2}$ peaks for specified samples. Samples: (bottom) Ag_2O film on Ag plate anodized at 0.3 V for 10 min in 0.1 M NaOH; (middle) AgO film on Ag plate anodized at 0.6 V for 10 min in 0.1 M NaOH; (top) oxide film on 1:20 (wt:wt) Ag-Pb alloy anodized at 0.9 V for 30 min in 0.1 M carbonate buffer (pH 10).

Scanning electron microscopy (SEM)

The binary phase diagrams for the Ag-Pb system show that Ag-Pb alloys prepared with Ag > 2.4% (by wt.) consist of two stable phases at room temperature: a eutectic phase containing 4.5% (at. %) of Ag, with the excess Ag existing as small Ag grains. Therefore, the surfaces of anodized Ag-Pb alloys containing > 2.4% Ag (by wt.) can be expected to consist of small islands of silver oxide within a surface matrix of the mixed silver-lead oxide. Figure 1.8 contains the SEM image (upper left) and elemental maps of the same surface region for an anodized Ag-Pb alloy containing 20% Ag (by wt.). Elemental maps correspond to the following: oxygen (upper right), lead (lower left), and silver (lower right). The intensity of the white spots in the silver elemental map is qualitative evidence of high local concentrations (islands) of silver oxide concluded above to be primarily AgO.

The data in Figure 1.8 are consistent with the existence of AgO islands (*ca.* 50-μm dia.) within an anodized Ag-Pb eutectic phase. As expected, SEM data (not shown) for an anodized Ag-Pb alloy containing 5% Ag (by wt.) revealed a significantly decreased population of AgO islands in comparison with Figure 1.8. Furthermore, SEM data (not shown) for the anodized Ag-Pb eutectic phase containing 2.4% Ag (by wt.) revealed a total absence of AgO islands.

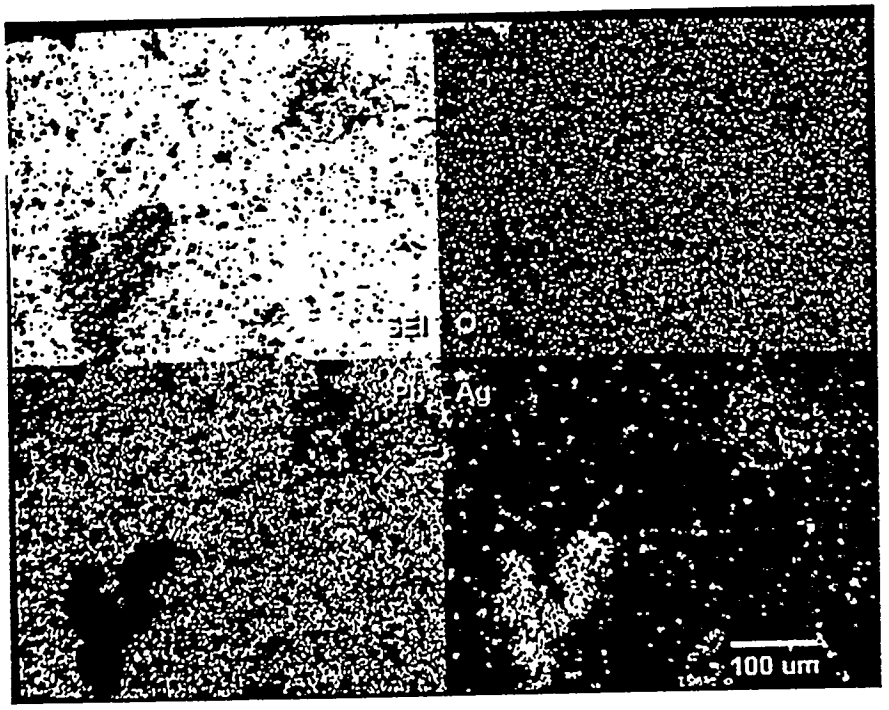

Figure 1.8. Scanning electron microscopic image and elemental maps for anodized 1:5 (wt:wt) Ag-Pb alloy. Upper left: total SEM image. Upper right: oxygen map. Lower left: lead map. Lower right: silver map.

Conclusions

Electrodes comprised of the anodized Ag-Pb alloys exhibit superior stability of response for aliphatic amines in comparison to electrodeposited Ag-Pb oxide films. Comparable voltammetric response is observed for representatives of primary, secondary and tertiary aliphatic amines, alkanolamines, and amino acids. The only organic product detected from oxidation of ethylamine and *L*-alanine is acetaldehyde. It is apparent, therefore, that the adjacent hydrophilic carboxyl group in the amino acid does not have a detrimental effect on the anodic response mechanism.

The catalytic activity of the anodized eutetic-phase Ag-Pb alloy electrodes for oxidation of amines is maintained in alkaline solutions of borate (pH 11) and phosphate (pH 12). However, no response was observed in neutral phosphate buffer (pH 7), presumably because protonation of the nitrogen in the amine groups blocks adsorption at the silver sites in the Ag-Pb oxide surface. Chloride added to the carbonate buffer attenuates the anodic response of aliphatic amines, presumably by blocking silver sites which normally function in the response mechanism for discharge of H_2O and for adsorption of amine groups. Amine response also is attenuated at large positive potentials because the corresponding large residual current from rapid discharge of H_2O with production of adsorbed hydroxyl radicals ($^{\cdot}OH_{ads}$) and subsequent evolution of O_2 at the silver sites is very effective in blocking amine adsorption which, therefore, blocks the anodic response mechanism. Addition of acetonitrile, acetaldehyde, acetone, and ethanol did not attenuate the amine signals; therefore, it is assumed these compounds are not

adsorbed at the silver sites.

Oxide films on anodized Ag-Pb alloy containing high levels of Ag (» 2.4% by wt.) yield XRD spectra characteristic of mixtures of PbO and AgO. XPS spectra of these same surfaces indicate the presence of AgO. SEM micrographs of these same surfaces indicate that the silver present in excess of the eutectic phase exists as islands of silver oxide, probably AgO, a surface matrix of the anodized eutectic phase. SEM data for the anodized eutectic phase gave no indication of the presence of AgO islands. XRD spectra for the anodized eutectic phase (2.4% Ag, by wt.) were consistent with PbO without evidence for AgO or a mixed-metal oxide phase.

The unique electrocatalytic activity of anodized Ag-Pb alloys under constant applied potential for anodic detection of aliphatic amines in alkaline media is expected to make these electrodes useful for amperometric detection in liquid chromatography. The preparation of these electrodes is simple and they exhibit very satisfactory stability. Future publications will describe the effects of elevated temperature on the response mechanisms and applications to chromatographic separations of aliphatic amines.

Acknowledgments

Ames Laboratory is operated for the U.S. Department of Energy by Iowa State University under Contract No. W-7405-ENG-82. The authors acknowledge James W. Anderegg for obtaining XPS data and Victor G. Young for XRD data.

Literature Cited

1. G. Horvai and E. Pungor, *Crit. Rev. Anal. Chem.*, **21**, 1 (1989).
2. D. C. Johnson, D. A. Dobberpuhl, R. E. Roberts and P. J. Vandeberg, *J. Chromatogr.*, **640**, 79 (1993).
3. I.-H. Yeo and D. C. Johnson, *J. Electrochem. Soc.*, **134**, 1973 (1987).
4. I.-H. Yeo, S. Kim, R. Jacobson and D. C. Johnson, *J. Electrochem. Soc.*, **136**, 1395 (1989).
5. N. A. Hampson, J. B. Lee, J. R. Horley and B. Scanlon, *Can. J. Chem.*, **47**, 3729 (1969).
6. J. B. Kafil and C. O. Huber, *Anal. Chim. Acta*, **175**, 275 (1985).
7. B. S. Hui and C. O. Huber, *Anal. Chim. Acta*, **134**, 211 (1982); **243**, 279 (1991).
8. M. Fleischmann, K. Korinek and D. Pletcher, *J. Electroanal. Chem.*, **31**, 39 (1971).
9. T. N. Morrison, K. G. Schick and C. O. Huber, *Anal. Chim. Acta*, **120**, 75 (1980).
10. B. S. Hui and C. O. Huber, *Anal. Chim. Acta*, **197**, 361 (1987).
11. W. Th. Kok, U. A. Th. Brinkman, and R. W. Frei, *J. Chromatogr.*, **256**, 17 (1983).
12. W. Th. Kok, H. B. Hanekamp, P. Box and R. W. Frei, *Anal. Chim. Acta*, **142**, 31 (1982).
13. K. Štulík, V. Pacáková, M. Weingart and M. Podolák, *J. Chromatogr.*, **367**, 311 (1986).
14. P. Luo, F. Zhang and R. P. Baldwin, *Anal. Chem.*, **63**, 1702 (1991).
15. S. Siggia and J. G. Hanna, *Quantitative Organic Analysis via Functional Groups*,

4th ed., John Wiley and Sons: New York; 535 (1979).

16. P. J. Vandeberg, J. L. Kawagoe and D. C. Johnson, *Anal. Chim. Acta*, **260**, 1 (1992).

17. J. S. Gordon and D. C. Johnson, *J. Electroanal. Chem.*, **365**, 267 (1994).

18. C. P. Wilde and M. Zhang, *J. Electroanal. Chem.*, **327**, 307 (1992).

19. J. E. Vitt and D. C. Johnson, *J. Electrochem. Soc.*, **139**, 774 (1992).

20. J.Koutecky and V. G. Levich, *Dokl. Akad. Nauk. SSSR*, **117**, 441 (1957); *Zh. Fiz. Khim.*, **32**, 1565 (1958).

21. H. Lund and M. M. Baizer, *Organic Electrochemistry: An Introduction and a Guide*, 3rd ed., Marcel Dekker: New York; 582, 601 (1991).

22. *International Center for Diffraction Data*, 1601 Park Lane, Swarthmore, PA (1992).

23. G. Schön, *Acta Chem. Scand.*, **27**, 24 (1973).

24. V. K. Kaushik, *J. Electron Spectrosc. Relat. Phenom.*, **56**, 273, (1991).

25. T. G. Clarke, N. A. Hampson, J. B. Lee, J. R. Morley, and B. Scanlon, *Can. J. Chem.*, **46**, 3437, (1968); B. Miller, *J. Electrochem. Soc.*, **117**, 491, (1970).

26. S. W. Gaarenstroom and N. Winograd, *J. Chem. Phys.*, **67**, 3500, (1977).

ELECTROCATALYSIS OF ANODIC OXYGEN-TRANSFER REACTIONS: OXIDATION OF AMMONIA AT ANODIZED AG-PB EUTECTIC ALLOY ELECTRODES

A paper published in the Journal of Electrochemical Society [1]

Jisheng Ge [2] and Dennis C. Johnson [2,3]

Abstract

Ammonia (NH_3) in alkaline media is oxidized to NO_3^- at anodized Ag-Pb eutectic alloy electrodes (2.4% Ag by weight). The anodic signal is diminished for $pH < ca.$ 8 and this attenuation is attributed to the protonation of NH_3 to form NH_4^+. Protonation of NH_3 is concluded to prevent adsorption of the NH_3 at silver sites in the electrode surface as the initial step in the electrocatalytic oxidation mechanism. For $pH > ca.$ 10, the anodic signal decreases with time because of the loss of NH_3 by volatilization. The heterogeneous rate constant for oxidation of NH_3 to NO_3^- is significantly smaller than that for oxidation of ethylamine (EA) to acetaldehyde and NH_3 ($k_{app,NH_3}/k_{app,EA} = ca.$ 0.2). Hence, NH_3 is concluded to be a product of ethylamine oxidation at a rotated disk electrode whereas acetaldehyde and NO_3^- are the final products of the exhaustive electrolysis of ethylamine.

---

[1] See J. Electrochem. Soc., 1995, 142(10), 3420.

[2] Graduate Student and Professor, respectively. Department of Chemistry and Ames Laboratory, Iowa State University, Ames, IA 50010.

[3] Author for correspondence.

Introduction

Previously, we reported that primary, secondary and tertiary (but not quaternary) aliphatic amines can be oxidized at the anodized eutectic-phase Ag-Pb alloy (2.4% Ag by weight) in alkaline media (pH *ca.* 10).[1] Acetaldehyde was detected as the organic product of the exhaustive electrolysis of ethylamine and the primary step in the anodic reaction for ethylamine was concluded to correspond to: [1]

$$CH_3\text{-}CH_2\text{-}NH_2 + 2\,OH^- \rightarrow CH_3\text{-}CHO + NH_3 + H_2O + 2\,e^- \qquad [1]$$

The reaction mechanism was speculated to be electrocatalytic in nature with adsorption of the amine group at silver sites in the electrode surface via the non-bonded electron pair of the nitrogen atom. Cleavage of the carbon-nitrogen bond occurs with transfer of oxygen to the carbon radical from an adsorbed hydroxyl radical (OH) generated at an adjacent site by concomitant anodic discharge of H_2O.

Subsequent research has demonstrated that NH_3 is oxidized also at the anodized Ag-Pb alloy electrodes, albeit at a rate significantly slower than that for the primary reaction given above. Details of that research are presented here.

Experimental

Chemicals

Chemicals were analytical grade and were used as received. Water was distilled and purified further in a NANOpure II system (SYBRON/Barnstead). Buffer solutions

were prepared from Na_2CO_3, $NaHCO_3$, K_3PO_4, $KHPO_4$ or KH_2PO_4. Solutions of NH_3 were prepared from $(NH_4)_2SO_4$ and NH_4HCO_3. Standard solutions of NO_3^- were prepared from $NaNO_3$.

Wire electrodes (*ca.* 1-mm diameter, 30-cm length, *ca.* 9-cm^2 area) and disk electrodes (0.20-cm^2 area) were fabricated from the eutectic phase Ag-Pb alloy (2.4% Ag by weight) according to the previous procedure.[1]

Instrumentation

Voltammetric data at the rotated disk electrode (RDE) were obtained in the manner described previously.[1] Exhaustive electrolysis was performed with stirring in (50 mL) of buffer under potentiostatic conditions maintained by a Model 551 potentiostat (ECO, Inc.) with a Pt-wire counter electrode. All potentials were controlled and are reported *vs.* a saturated calomel electrode (SCE, Fisher Scientific). Temperature of solutions in a water-jacked cell was maintained at 25°C using by passage of water from a LAUDA thermostatic bath (Brinkmann). Values of *pH* were measured by a JENCO digital meter (Electronics, Ltd.) using a combination electrode calibrated at *pH* 7.00.

Ion chromatography was achieved using a PAX-500 "guard" column (4 mm x 5 cm; Dionex). The suppressor column was a polystyrene, high capacity, cation-exchange column (4 mm x 25 cm; Dionex) loaded in H^+-form by elution with 1 M H_2SO_4. The mobile phase was 2.0 mM $NaHCO_3$/2% MeCN pumped at a flow rate 1.0 mL min^{-1} by a Model GMP gradient pump (Dionex) operated in the isocratic mode. Conductometric detection was achieved with a Model 213 detector (Wescan Instruments) interfaced to a

desktop computer (IBM) via a DT2801 data acquisition board (Data Translation) using ASYST-3.1 software (Keithley/Asyst).

Nuclear magnetic resonance (NMR) spectrometry was performed with a Model DRX-400 spectrometer (Bruker), equipped with the UXNMR data system, using a ^{15}N-probe to identify the form of ^{15}N-enriched nitrogen product from exhaustive electrolysis. Transients were accumulated over a 24-kHz range using 16K words of memory. All spectra were phase corrected to display upright signals for easy presentation. The standard sample was 1.5 M $^{15}NH_4{}^{15}NO_3$/1 M HCl in D_2O in a 10-mm tube. Chemical shifts were recorded with respect to the N-peak for NH_4^+ as the reference.

Calculations

The fraction of total dissolved ammonia existing as NH_3 was calculated as a function of solution pH according to:

$$f_{NH_3} = \frac{K_w}{K_w + K_b(10^{-pH})} \qquad [2]$$

where K_w = 1.0 x 10^{-14} is the dissociation constant for H_2O at 25°C and K_b = 1.77x10^{-5} is the base dissociation constant for NH_3 at 25°C, as indicated by: [6]

$$NH_3 + H_2O \rightleftharpoons NH_4^+ + OH^- \qquad [3]$$

The effective number of electrons (n_{eff}, eq mol^{-1}) transferred during oxidation at the RDE were estimated from the slopes of linear plots of $1/i$ vs. $1/\omega^{1/2}$ according to the so-called Koutecky-Levich equation given by:[2]

$$1/i_{net} = 1/n_{eff}FA_{geo}k_{app}C^b + 1/0.62n_{eff}FA_{geo}D^{2/3}\nu^{-1/6}C^b\omega^{1/2} \quad [4]$$

where i_{net} is the net electrode current (mA) corrected for the background response (i_{tot} – i_{bkg}), A_{geo} is the geometric area of the disk electrode (cm^2), k_{app} is the apparent heterogeneous rate constant (cm s^{-1}), ν is the kinematic viscosity of the solution (cm^2 s^{-1}), C^b is the bulk concentration of the reactant (mol L^{-1}), and F and D have their usual electrochemical significance. It is important to recognize that derivation of the Koutecky-Levich equation assumes that the transfer of n_{eff} electrons occurs as a single step at a rate constant of k_{app}.

Results and Discussion

Voltammetric Response

Anodic response for NH_3 is observed at anodized Ag-Pb eutectic alloy electrodes (2.4% Ag by weight) in the potential region corresponding to onset of anodic discharge of H_2O. This fact is illustrated in Figure 2.1 for 1.0 mM $(NH_4)_2SO_4$ as a function of rotational velocity in carbonate buffer (pH *ca.* 10). Whereas this test solution was prepared from $(NH_4)_2SO_4$, results of a pH study described below support the conclusion

that the species being oxidized is NH_3 and this designation of the electroactive species is used from the outset in this report.

It is apparent in Figure 2.1 that the net current response for NH_3 ($i_{net} = i_{tot} - i_{bkg}$) has a slight peaked shape. This peaked response apparent for the positive potential scan in Figure 2.1 is retraced during the subsequent negative scan (data not shown). Hence, the peaked response for NH_3 is not a consequence of surface fouling by some irreversibly adsorbed oxidation product. A peaked response also was reported for aliphatic amines [1] and was concluded to be the result of the dual role of the silver sites in the mixed-oxide surface. This same explanation is offered here to explain the peaked response observed for NH_3. Accordingly, the silver sites function catalytically for adsorption of NH_3 molecules within the oxidation mechanism. However, as the potential is increased, these same silver sites also begin to function for the anodic discharge of H_2O to produce adsorbed hydroxyl radicals (OH_{ads}). These OH_{ads} species compete with NH_3 for the silver sites and, thereby, cause the observed attenuation of the NH_3 signal as the rate of H_2O discharge increases with increasing potential. It is apparent also from Figure 2.1 that the potential corresponding to the peak value of net anodic response ($i_{net,p}$) is shifted to more positive values as the flux of NH_3 is increased. This flux increase can be achieved by increasing the rotational velocity of the disk electrode, as illustrated in Figure 2.1, or by increasing the concentration of NH_3 (data not shown). The positive shift in peak potential can be explained as the result of the requirement of an increased OH_{ads} flux, i.e., more positive potential, as the flux of NH_3 is increased. A similar shift in the peak value of i_{net} was reported for ethylamine.[1]

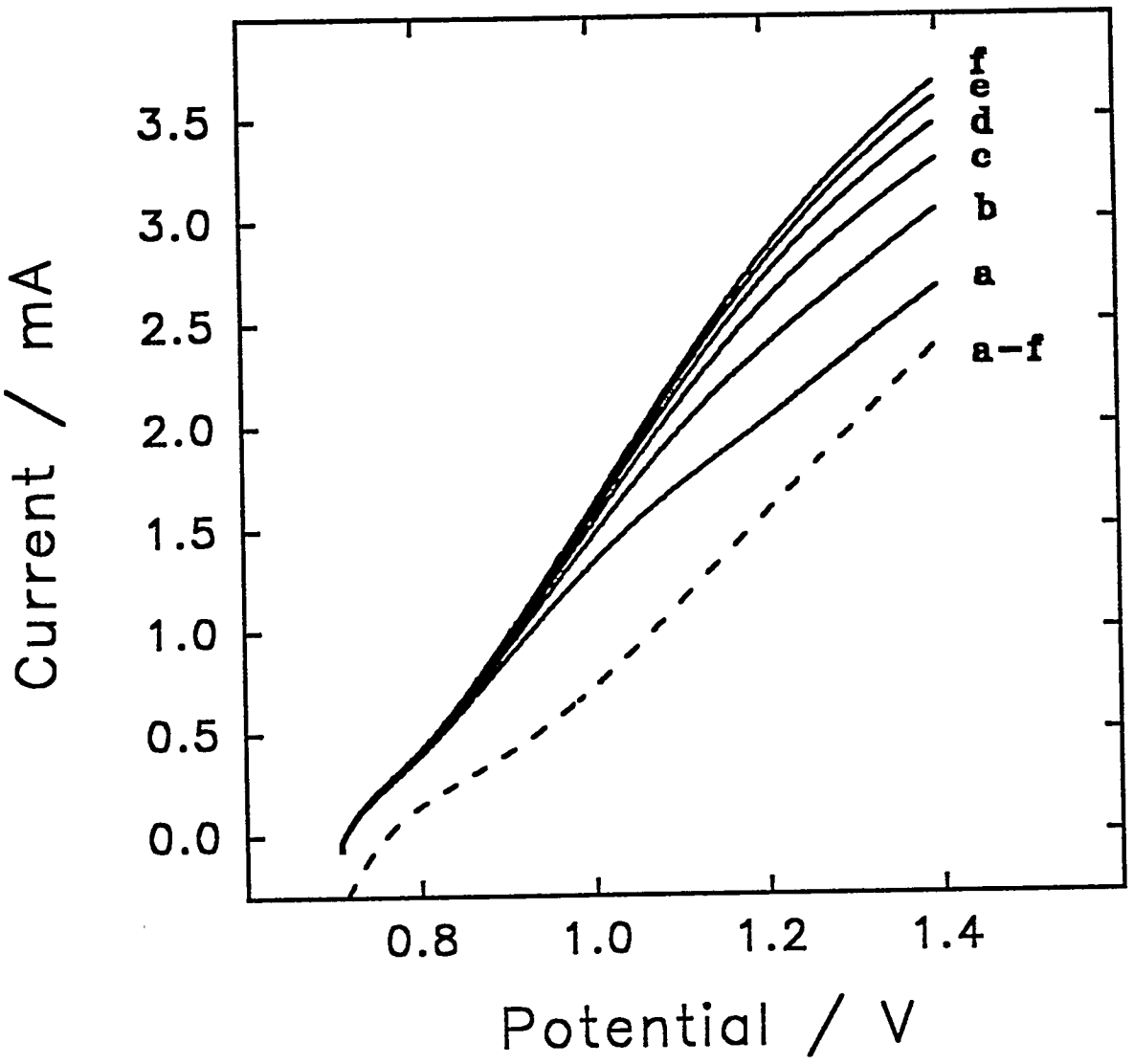

Figure 2.1. Voltammetric responses (pos. scan) for $(NH_4)SO_4$ at an anodized eutectic-phase Ag-Pb alloy disk electrode as a function of rotation speed in 0.1 M carbonate buffer (pH 10). Scan rate: 2.0 V min^{-1}. Concentration of $(NH_4)_2SO_4$ (mM): (- - - -) 0, (——) 1.0. Rotational velocity (rad s^{-1}): (a) 42, (b) 94, (c) 168, (d) 262, (e) 377, (f) 513.

Koutecky-Levich plots made for the peak value of the net current ($1/i_{net,p}$ *vs.* $1/\omega^{1/2}$) are shown in Figure 2.2 for 2.0 mM ethylamine (●) and 2.0 mM NH_4HCO_3 (▽) in 0.1 M carbonate buffer (pH 10). These plots are linear, with the following values of intercept (*a*), slope (*b*), and regression coefficient (*r*). For ethylamine (EA): $a = 0.764$ mA^{-1}, $b = 22.8$ mA^{-1} rad$^{1/2}$ s$^{-1/2}$, and $r = 0.9994$. For NH_3: $a = 0.970$ mA^{-1}, $b = 5.17$ mA^{-1} rad$^{1/2}$ s$^{-1/2}$, and $r = 0.9993$. The value $n_{eff,EA} = 1.8$ eq mol^{-1} is estimated from the slope of the Koutecky-Levich plot for EA using the value $\nu = 7.53 \times 10^{-3}$ cm^2 s^{-1} [3] and the generic estimate $D = 1 \times 10^{-5}$ cm^2 s^{-1}. This value of $n_{eff,EA}$ is somewhat smaller than the value 2 eq mol^{-1} for production of acetaldehyde and NH_3 according to Equation [1]. This lack of agreement might be the result of an inaccurate estimate for *D*. The value $n_{eff,NH_3} = 6.2$ eq mol^{-1} is estimated from the slope of the Koutecky-Levich plot for NH_3 in Figure 2.2 using $\nu = 7.53 \times 10^{-3}$ cm^2 s^{-1} [3] and $D = 1.42 \times 10^{-5}$ cm^2 s^{-1} for NH_4^+.[4] In another experiment, the value $n_{eff,NH_3} = 8.4$ eq mol^{-1} was estimated from the Koutecky-Levich plot for 2.0 mM $(NH_4)_2SO_4$. These values are considered to be in fair agreement with the conclusion that NH_3 is oxidized to NO_3^- according to:

$$NH_3 + 9\,OH^- \rightarrow NO_3^- + 6\,H_2O + 8\,e^- \qquad [5]$$

The high variability apparent in experimental values for n_{eff,NH_3} probably is a consequence of error in the value used for C^b in these calculations as a consequence of the volatility of NH_3 at high pH.

The ratio of slopes for Koutecky-Levich plots for ethylamine and NH_3 in Figure 2.2 is 22.8/5.17 = 4.4. This is in fair agreement with the ratio $n_{eff,NH_3}/n_{eff,EA} = 4$ predicted

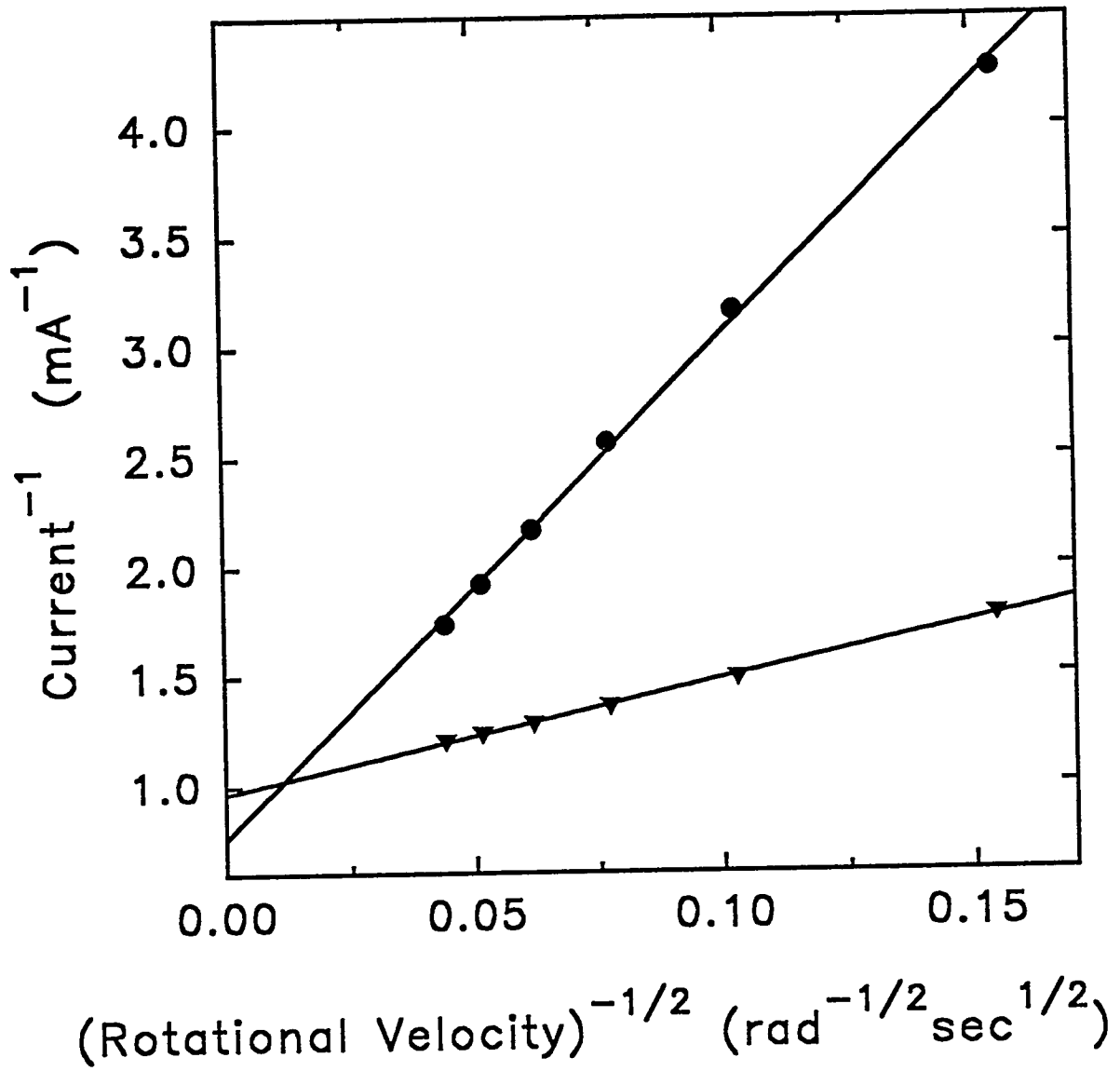

Figure 2.2. Koutecky-Levich plots for voltammetric peak responses for (▽) 2.0 mM NH_4HCO_3 and (●) 2.0 mM ethylamine in 0.1 M carbonate buffer (pH 10). Scan rate: 2.0 V min^{-1}.

on the basis of Equations [1] and [5], with the assumption of equal values of D for the two electroactive species. The tendency for NH_3 to be lost from the solution by volatilization at pH 11.5 causes this ratio to increase with time because the initial value of $C^b_{NH_3}$ = 2.0 mM was used in the calculation.

The values of C^b for ethylamine and NH_3 were approximately the same in experiments generating the data for the Koutecky-Levich plots shown in Figure 2.2. Therefore, the ratio of these intercepts is useful for an approximately comparison of the k_{app} values for the two oxidation reactions. Accordingly, we calculate 0.764/0.970 = $n_{eff,NH_3}k_{app,NH_3}/n_{eff,EA}k_{app,EA}$ = *ca.* 0.79. Using, $n_{eff,NH_3}/n_{eff,EA}$ = 8/2, we calculate $k_{app,NH_3}/k_{app,EA}$ = 0.79(2/8) = 0.20. . Hence, the primary reaction for oxidation of ethylamine at the RDE according to Equation (1) is significantly faster than the oxidation of NH_3. Therefore, the products of oxidation of primary amines at the RDE can be correctly concluded to be acetaldehyde and NH_3 (n_{eff} = 2 eq mol^{-1}), with relatively little oxidation of NH_3; whereas the final products of exhaustive electrolysis are acetaldehyde [1] and probably NO_3^-. Aldehydes are not reactive at the Ag-Pb alloy electrode.

pH Effects

As speculated previously for oxidation of aliphatic amines, [1] we speculate here also for oxidation of NH_3 at Ag-Pb alloy electrodes that NH_3 is adsorbed at silver sites in the mixed-oxide surface via formation of coordination bonds with the non-bonded electrons of the nitrogen atom. Thus, for acidified media ($pH < pK_w/pK_a$), the anodic

response is predicted to be attenuated as a consequence of protonation of the non-bonded electrons on the nitrogen atom.

Shown in Figure 2.3 are values of f_{NH_3} calculated as a function of pH according to Equation 2. Also shown are values of $i_{net,p}$ as a function of pH. It is observed in Figure 2.3 that $i_{net,p}$ increases from ca. 0 mA at pH 4 (f_{NH_3} = ca. 0) to 0.4 mA at pH 8 (f_{NH_3} = 0.5). The observation supports the conclusion that NH_3 and not NH_4^+ is the species detected at the electrode. However, for values of $pH > 9.5$ ($f_{NH_3} > 0.7$), $i_{net,p}$ is observed to decrease abruptly. Furthermore, values of $i_{net,p}$ were observed to steadily decrease with time for $pH > 9.5$. This loss of anodic signal is concluded to occur because of the loss of volatile NH_3 from the cell. More specifically, the value of $i_{net,p}$ obtained at the RDE (168 rad s^{-1}) was observed to decrease from its initial value by 40% within 5 min and 60% within 10 min. The data shown in Figures 2.1 and 2.2 for the NH_3 response at pH 10 were obtained very quickly (< 2 min) after addition of the $(NH_4)_2SO_4$ and NH_4HCO_3, respectively, to minimize losses of NH_3 by volatilization.

Additional evidence for the importance of adsorption of NH_3 molecules at catalytic silver sites in the mixed-oxide surface is the observation that addition of 10 mM Cl^- resulted in a 56% decrease in NH_3 signal. Undoubtedly this occurs because Cl^- is adsorbed at the silver sites and, thereby, blocks adsorption of NH_3.

Product Identification

Anion-exchange chromatography with conductometric detection was applied for the qualitative and quantitative analysis of product solutions from the exhaustive electrolysis

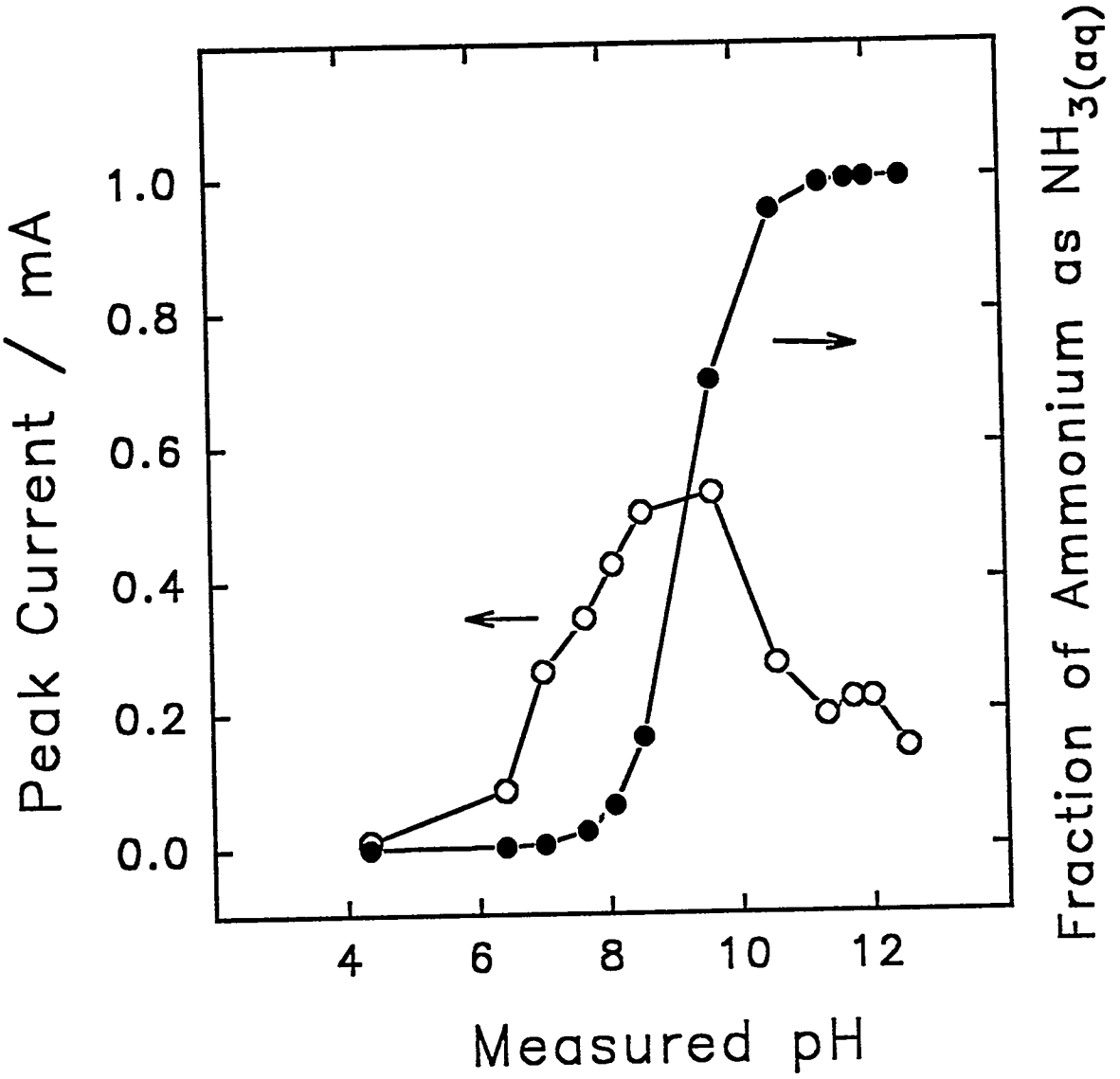

Figure 2.3. Correlation of voltammetric peak response and calculated concentration of $NH_3(aq)$ as a function of pH. Buffer: 50 mM NaH_2PO_4 adjusted to pH by NaOH. Scan rate: 2.0 V min^{-1}. Rotational velocity: 168 rad s^{-1}.

of NH_4HCO_3 in 0.1 M carbonate buffer (pH 8.5). Use of NH_4HCO_3 instead of $(NH_4)_2SO_4$ avoided the introduction of SO_4^{2-} which could complicate the chromatographic results. The electrolysis cell was enclosed to minimize loss of NH_3 by volatilization during the extended electrolysis periods. Chromatographic separations were achieved using a short (4 mm x 5 cm) commercial column exhibiting both ion-exchange and reverse-phase retention mechanisms. Of the various mobile phases tested, 2 mM $NaHCO_3$/2% MeCN (pH 8.5) was determined to give adequate separation of peaks from NO_2^-, NO_3^-, HCO_3^- and CO_3^{2-} (see Table 1). The chromatographic system was standardized using NO_3^- solutions with concentration in the range 10 to 50 μM. Peak height for NO_3^- was

Table 1. Retention times and capacity factors for NO_2^-, NO_3^-, HCO_3^- and CO_3^{2-} separated by anion-exchange chromatography.

Anion	Concentration [a] (μM)	Retention time	Capacity factor (k′)
NO_2^-	30	1′49″	0.54
HCO_3^-	1000	2′13″	0.87
CO_3^{2-}	250	2′13″	0.87
NO_3^-	30	3′14″	1.73

[a] Injection volume: 50 μL.

[b] Mobile phase: 2 mM $NaHCO_3$/2% MeCN @ 1.0 mL min^{-1}.

determined to be a linear function of concentration with a sensitivity of 0.389 cm μM^{-1}, a standard error of estimate ($s_{y/x}$) of 0.133 cm μM^{-1}, and a correlation coefficient (r) of 0.9998. The detection limit was *ca.* 0.1 μM NO_3^- (S/N = 3).

Exhaustive electrolysis was performed for a 50-ml solution of 100 mm NH_4HCO_3 in 0.2 M carbonate buffer (ph 8.5). Small aliquots (50 μL) of the product mixture were diluted 100 times with deionized water and then injected into the chromatograph at fixed time interval during the course of the electrolysis. Representative chromatograms are shown in Figure 2.4 corresponding to electrolysis periods of (a) 1 hr, (b) 2 hr and (c) 5 hr. It is apparent that NO_3^- is the only product detected from the electrolysis reaction. Whereas this result supports the conclusion that NO_3^- is the water soluble product of NH_3 oxidation, these data cannot be the basis for eliminating the possibility that small amounts of volatile products are formed (e.g., N_2 and NO).

The chromatographic peak signal for NO_3^- increased linearly with time during the initial 10-hr electrolysis period. Negative deviation from linearity was observed for t > 10 hr, as is expected for exhaustive electrolysis. At t = 25 hr, the NO_3^- concentration had reached 85% of the theoretical yield based on the reaction in Equation [3]. Becauseof the slow rate of electrolysis and the very long time period required to achieve complete electrolysis (>> 25 hr), the time-integral of the *i-t* curve could not be used reliably for the estimation of n_{eff} in this oxidation reaction.

Verification that NO_3^- is the identity of the major product from the oxidation of NH_3(aq) was achieved using ^{15}N-NMR applied to the product solution from exhaustive

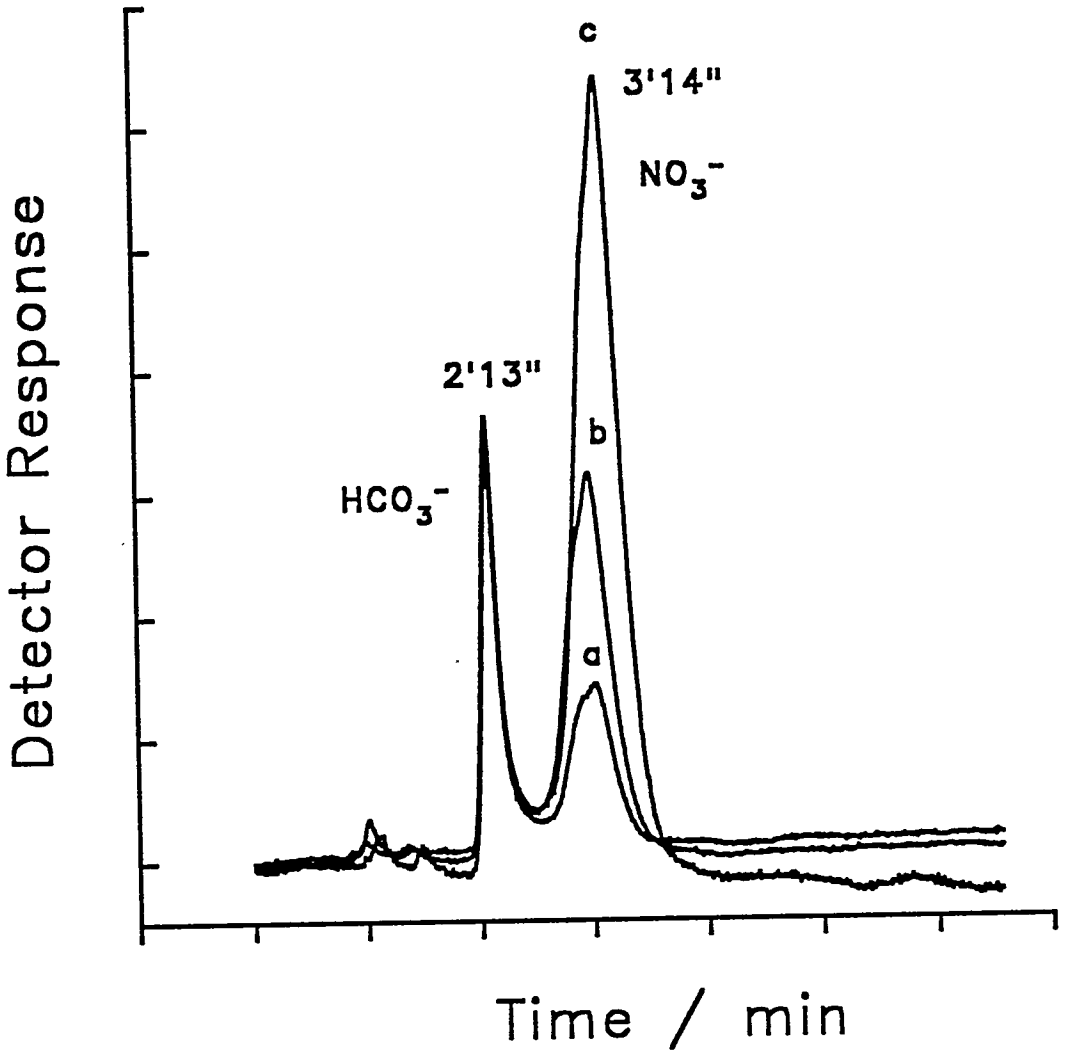

Figure 2.4. Ion chromatography results. Separation column: PAX-500 "guard" (4 mm x 5 cm). Suppressor column: strong-acid cation-exchange resin in H^+-form. Mobile phase: 2 mM $NaHCO_3$/2% MeCN @ 1.0 mL min^{-1}. Detection: conductivity. Wire electrode (*ca.* 9 cm^2): anodized eutectic-phase Ag-Pb alloy. Potential: 1.25 V vs. SCE. Solution: 4.93 mmol NH_4HCO_3 in 50 mL 0.2 M carbonate buffer (pH 8.5). Electrolysis time (hr): (a) 1.0, (b) 2.0, (c) 5.0.

electrolysis of ^{15}N-enriched $(NH_4)_2SO_4$. The NMR peak of NO_3^- (355.5 ppm) is considered to be an excellent match for that obtained for the NH_4NO_3 standard (351.6 ppm). This small difference in shift is attributed to a small difference in pH between the two solutions.

Based on these results, we conclude the overall oxidation of ethylamine for exhaustive electrolysis at the Ag-Pb alloy electrode is given by:

$$CH_3\text{-}CH_2\text{-}NH_2 + 11\,OH^- \rightarrow CH_3\text{-}CHO + NO_3^- + 7\,H_2O + 10\,e^- \qquad [6]$$

Chronoamperometry

The chronoamperometric response (*i-t*) is shown in Figure 2.5 obtained during exhaustive electrolysis of 17.5 mM ethylamine (curve b) in 0.1 M carbonate buffer (*pH* 10) using an enclosed electrolysis cell with magnetic stirring. Curve a corresponds to the background response in the absence of ethylamine. This background current is primarily the result of formation of some additional surface oxide immediately upon application of the constant potential and continuous anodic discharge of H_2O with evolution of $O_2(g)$. It is very evident from curve b that the response for ethylamine is not correspond with a simple first-order decay process as is expected in exhaustive electrolysis wherein the electrode reaction corresponds to the reaction of a single species occurring with the transfer of a constant number of electrons. The response for ethylamine can be explained on the basis of the conclusion above that $k_{app,EA}$ for the primary step in the oxidation of ethylamine (n_{app} = 2 eq mol^{-1}) is significantly larger than k_{app,NH_3} for oxidation of NH_3 (n_{app} = 8 eq mol^{-1}). Accordingly, the initial response (t = 0) corresponds to n_{net} = *ca.* 2 eq mol$^-$

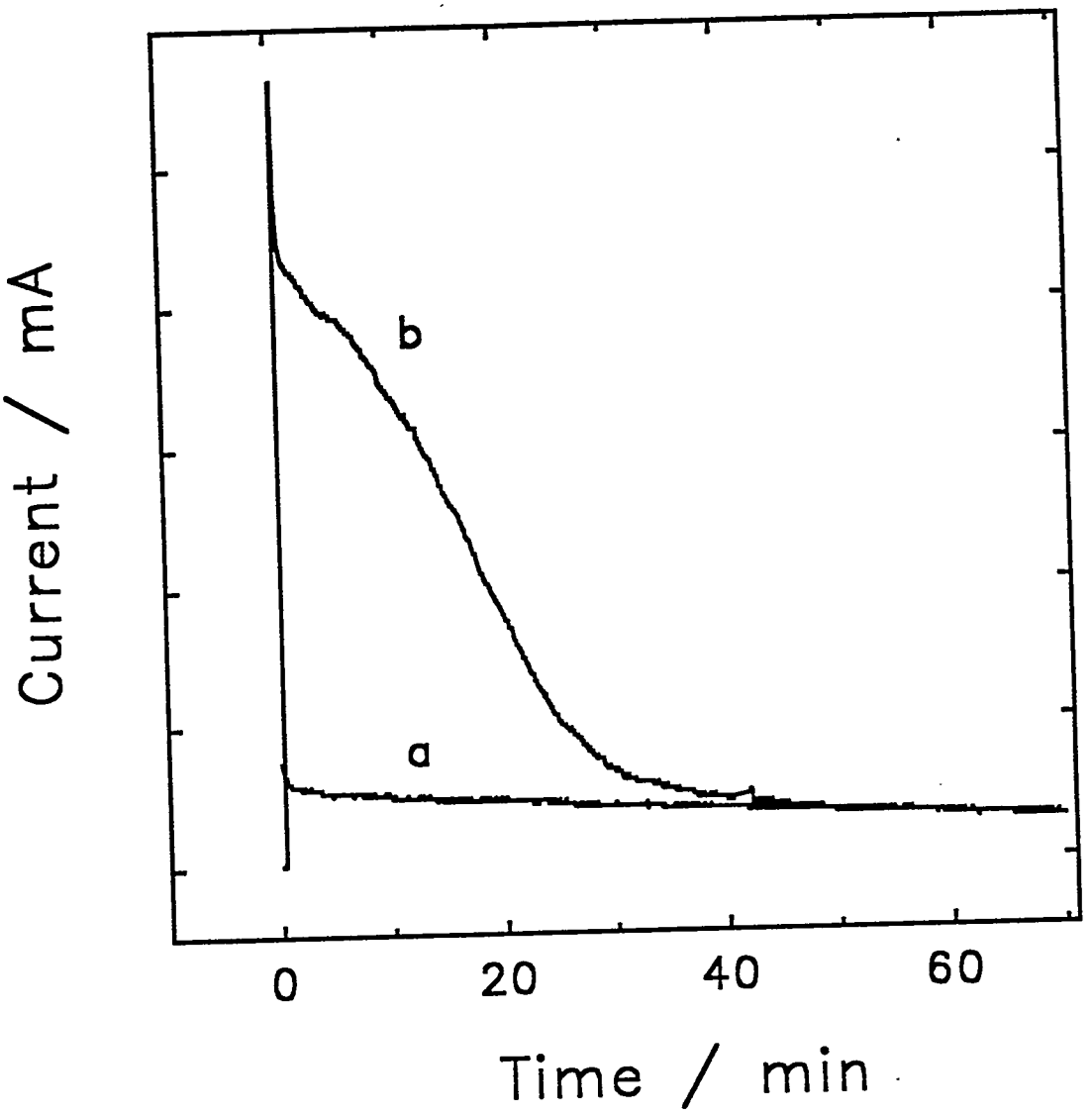

Figure 2.5. Current-time profiles for the exhaustive electrolysis of ethylamine in stirred 0.1 M carbonate buffer (pH 10). Wire electrode (*ca.* 9 cm^2): anodized eutectic phase of Ag-Pb alloy. Potential: 1.0 V vs. SCE. Curves: (a) residual, (b) 17.5 mM $(NH_4)_2SO_4$.

[1]. Immediately thereafter ($0 < t \ll \infty$), the concentration of NH_3 increases concomitantly with the decrease in ethylamine concentration. Hence, because $n_{eff,NH_3} > n_{eff,EA}$, the current-time response deviates from a simple first-order decay curve. Finally ($t \rightarrow \infty$), when ethylamine has been depleted from the solution, n_{net} becomes constant at the value n_{eff,NH_3} and the shape of the current-time curves is as expected for a first-order decay.

Conclusions

The product of exhaustive electrolysis of NH_3 at a Ag-Pb alloy wire electrode is NO_3^- and the reaction is concluded to correspond to that given by Equation 5 (8 eq mol^{-1}). This is consistent with the values n_{eff,NH_3} = 6.2 and 8.4 eq mol^{-1} calculated from the slopes of Koutecky-Levich plots for oxidation of NH_3 at a Ag-Pb rotated disk electrode (RDE).

The products from exhaustive electrolysis of ethylamine at Ag-Pb alloy wire electrodes are acetaldehyde and NO_3^-, which is consistent with the reaction given by Equation 6 (10 eq mol^{-1}). However, the value $n_{eff,EA}$ = 1.8 eq mol^{-1} is calculated, using a generic value for the diffusion coefficient, on the basis of the slope of the Koutecky-Levich plot for ethylamine at a RDE. Hence, we conclude, for conditions of rapid convective-diffusional mass transport at the RDE, that there is relatively little contribution to the total current observed for ethylamine coming from further oxidation of the NH_3 produced by the primary step in the oxidation reaction for ethylamine.

These conclusions can be rationalized on the basis of a significantly faster heterogeneous rate constant for the primary step in ethylamine oxidation as compared with

that for NH_3 ($k_{app,NH_3}/k_{app,EA}$ = *ca.* 0.2) calculated from the intercepts of the respective Koutecky-Levich plots. This observation that $k_{app,EA} > k_{app,NH_3}$ can be rationalized on the basis of fact that the C-N bond energy (286 kJ mol^{-1}) is significantly smaller than the N-H bond energy (391 kJ mol^{-1}).[8]

Oswin and Salomon studied the oxidation of NH_3 to N_2 on Pt electrodes.[7] They proposed formation of the surface species Pt-NH_2, Pt=NH and Pt≡N as intermediate products in the electrocatalytic mechanism. They speculated that the final reaction step is the combination of two N-atoms from adjacent Pt≡N species to form N_2. If N-atoms are adsorbed at the widely separated silver sites, as is characteristic of the Ag-Pb alloy electrode surfaces containing a small amount of Ag, then formation of N_2 is kinetically unfavorable. Therefore, the formation of N_2 can be understood not to be a significant competing reaction in the anodic mechanism at Ag-Pb alloy electrodes that achieves the transfer of oxygen atoms from OH_{ads} on surface sites adjacent to the adsorbed N-species to achieve production of NO_3^-.

Acknowledgments

Ames Laboratory is operated for the U.S. Department of Energy by Iowa State University under Contract No. W-7405-ENG-82. The ^{15}N NMR data were obtained by R.D. Scott.

List of References

1. J. Ge and D. C. Johnson, *J. Electrochem. Soc.*, accepted.
2. J. Koutecky and V. G. Levich, *Dokl. Akad. Nauk. SSSR*, **117**, 441 (1957); *Zh. Fiz. Khim.*, **32**, 1565 (1958).
3. C. S. Pac, I. M. Maksimova and L. V. Glushenko, *J. Phys. Chem. USSR*, **57**, 846 (1984).
4. J. G. Albright, J. P. Mitchell and D. G. Miller, *J. Chem. Eng. Data*, **39**, 195 (1994).
5. T. G. Clarke, N. A. Hampson, J. B. Lee, J. R. Morley and B. Scanlon, *Can. J. Chem.*, **46**, 3437 (1968). B. Miller, *J. Electrochem. Soc.*, **117**, 491 (1970).
6. F. Albert Cotton and Geoffrey Wilkinson, *Advanced Inorganic Chemistry*, 5th ed., John Wiley & Sons: New York, (1988) p. 314.
7. H. G. Oswin and M. Salomon, *Can. J. Chem.*, **41**, 1686 (1963); A. R. Despić, D. M. Dražić and P. M. Rakin, *Electrochim. Acta*, **11**, 997 (1966).
8. D. A. Johnson, *Some Thermodynamic Aspects of Inorganic Chemistry*, 2nd ed., Cambridge University Press: Cambridge, England (1982) p.201.

ELECTROCATALYSIS OF ANODIC OXYGEN-TRANSFER REACTIONS: TEMPERATURE EFFECTS ON OXIDATION OF ETHYLAMINE, ALANINE AND AMMONIA AT ANODIZED AG-PB EUTECTIC ALLOY ELECTRODES

A paper to be submitted for publication in the Journal of the Electrochemical Society

Jisheng Ge and Dennis C. Johnson

Abstract

Values of the activation energy (ΔH°_{act}) for oxidation of ethylamine and alanine are estimated to be 17.1 and 7.17 kJ mol^{-1}, respectively, from temperature effects on the apparent heterogenous rate constants estimated from Koutecky-Levich plots for anodized Ag-Pb eutectic disk electrodes in carbonate buffer (pH 10). The value of ΔH°_{act} for oxidation of aquated ammonia is estimated to be 38.5 kJ mol^{-1} from data obtained in a flow-through reactor. The correlations of peak potentials for ethylamine with overpotentials for anodic evolution of O_2 as a function of temperature is interpreted on the basis of the coupling of these anodic processes via the adsorbed hydroxyl species (OH) produced by anodic discharge of H_2O.

Introduction

Previous research at ambient temperature (ca. 25 °C) has demonstrated that anodized eutectic-phase Ag-Pb alloy electrodes exhibit electrocatalytic activity for anodic oxidation of a variety of aliphatic amines in alkaline media. Included are primary, secondary and tertiary

(but not quaternary) amines, amino acids and alkanolamines. The oxidation of ethylamine was determined to produce ethylaldehyde and ammonia by a rapid reaction given by:[1]

$$CH_3\text{–}CH_2\text{–}NH_2 + 2\,OH^- \longrightarrow CH_3\text{–}CHO + NH_3 + H_2O + 2\,e^- \qquad (1)$$

This is followed by the slow oxidation of NH_3 to NO_3^- with the overall reaction for exhaustive electrolysis given by:[2]

$$CH_3\text{–}CH_2\text{–}NH_2 + 11\,OH^- \longrightarrow CH_3\text{–}CHO + NO_3^- + 7\,H_2O + 10\,e^- \qquad (2)$$

Ethylaldehyde also was determined to be produced in exhaustive electrolysis of alanine and the rapid initial step for alanine was concluded to be given by:[1]

$$CH_3\text{–}CH_2NH_2\text{–}COO^- + OH^- \longrightarrow CH_3\text{–}CHO + CO_2 + NH_3 + 2\,e^- \qquad (3)$$

One consequence of the kinetic complexity for the overall reaction is expected to be a high temperature sensitivity for the voltammetric response. More specifically, the effective number of electrons transferred (n_{eff}) for oxidation of an amine might deviate significantly from the value 2 eq mol^{-1} for a large temperature variation about 25 °C. Previously, Hui and Huber[3] demonstrated that the response for oxidation of several amino acids at anodized Ni electrodes is very sensitive to temperature variations.[3] Results are described here for a temperature study of the anodic response for ethylamine, alanine and ammonia. Also given is an explanation for the variation of the potential of peak response for amines at a disk electrode as a function of rotational velocity and amine concentration.

Experimental

Reagents

Chemicals were analytical grade. Water was distilled followed by purification in a NANO-pure-II system (Barnstead). Supporting electrolyte was 0.10 M $NaHCO_3$-Na_2CO_3 buffer adjusted to pH 10.0. Stock solutions of ethylamine were prepared by dissolution of the commercial reagent in purified water with standardization by acidimetric titration. [1]

Equipment

Voltammetric data were obtained at a rotated disk electrode (RDE) assembled from an anodized eutectic Ag-Pb alloy disk [1] and mounted in an ASR rotator (Pine Instrument Co.). Potentiostatic control was provided by a RDE3 potentiostat (Pine). The jacketed electrochemical cell was constructed from Pyrex with the reference and counter electrodes located in compartments separated from the working compartment by fritted glass disks (medium porosity). Temperature control of the working compartment was achieved by thermostated water (±0.1 °C) flowing through the water jacket from a Lauda K-2/RD refrigerated/heated circulating bath (Brinkmann Instruments). The reference electrode was a miniature saturated calomel electrode (SCE, Fisher Scientific) and all potentials are given with respect to the SCE.

Figure 3.1 contains a schematic diagram of the flow-through electrolytic reactor used for electrolysis of NH_3. The jacketed electrolysis chamber was constructed from pyrex tubing (30-cm long, 1-cm i.d.) with a thermometer (T) inserted in one end and an anodized Ag-Pb alloy working electrode (W) (2-mm diameter, 28-cm length, 17.6-cm^2 area) inserted

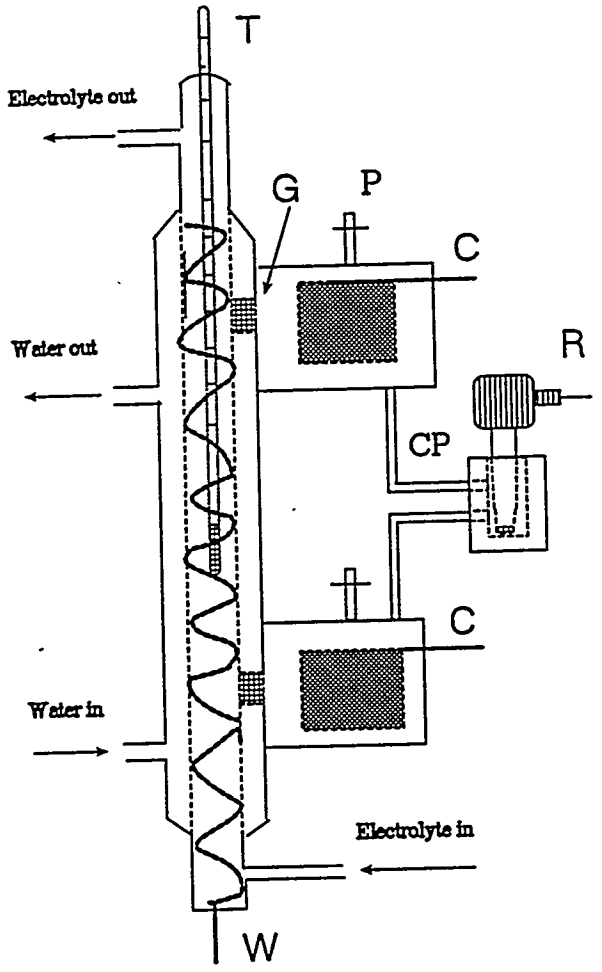

Figure 3.1. Schematic diagram of water-jacketed flow-through electrolysis reactor. Components: (C) counter electrodes, (G) fritted glass disks, (R) reference electrode, (W) working electrode, (CP) capillary tube, (P) pressure valve, (T) thermometer.

through the other end. Two compartments containing Pt-screen counter electrodes (C) (*ca.* 126-cm^2 area) were attached to the jacketed tube by fritted glass disks (G). Each counter-electrode compartment was equipped with a pressure valve (P) to release H_2(g) generated by the cathodic reactions at the counter electrodes. The SCE reference (R) was attached to the counter electrode compartments by plastic tubing (CP) (0.63-mm i.d., Elkay Products). The temperature in the working compartment was controlled by thermostated water pumped through the jacket by the LAUDA bath. The reference and counter electrode compartments were maintained at ambient temperatures. Working electrode potential in the reactor was controlled by Model 551 potentiostat (PS) (ECO, Inc.).

Figure 3.2 illustrates the coupling between the flow-through reactor (Figure 3.1) with an ion chromatograph. Electrolyte and reactant were pumped through the reactor at controlled flow rates by a model EVA pump (P1) (Eppendorf). Product solution from the reactor was sample by a model 7010 six-port injection valve (V) (Rheodyne) having a 25-μL sample loop. Samples were passed through OmniPac PAX-500 guard (G) (4 mm x 5 cm) and analytical (A) (4 mm x 25 cm) columns (Dionex). The mobile phase was 5 mM carbonate buffer (pH 10) with 5% acetonitrile[4] and delivered from a model GMP pump (P2) (Dionex). Anion suppression was achieved with a model ASRS-I self-generating membrane suppressor (S) (Dionex) with a regenerant consisting of 50 mm H_2SO_4 (5 mL min^{-1}) from a model AMP-1 pump (P3) (Dionex). Conductivity detection was achieved by a model 213 detector (D) (Wescan). Use of 0.1 M carbonate buffer (pH 10) circumvented troublesome interferences by impurity anions. Injection of solutions from the reactor resulted in chromatographic peaks only for carbonate (180 s) and nitrate (310 s) ions. The peak

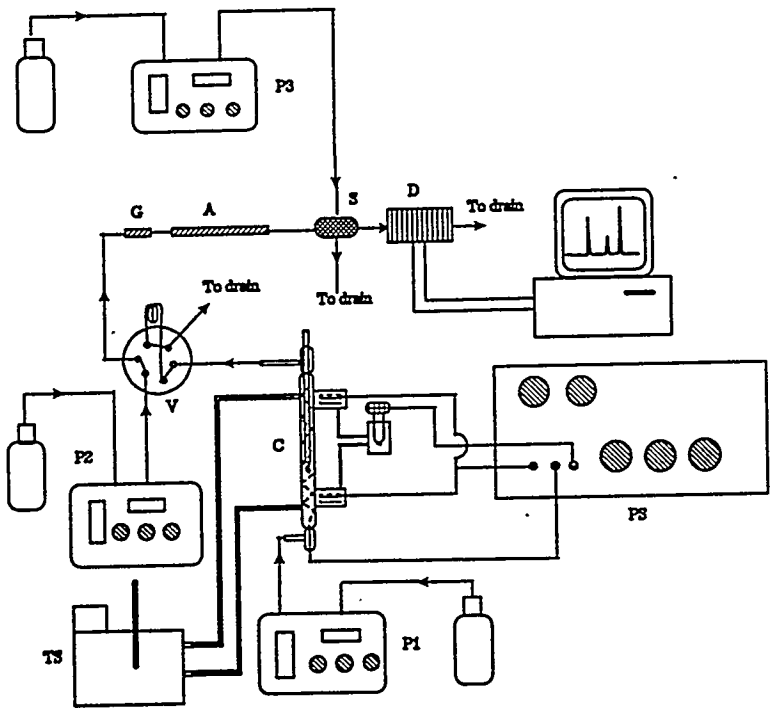

Figure 3.2. Schematic diagram of the interface between the flow-through reactor and the Ion Chromatography. Components: (P1) pump-1, (P2) pump-2, (P3) pump-3, (C) flow-through reactor, (TS) thermostat, (V) valve, (G) guard column, (A) analytical column, (S) suppressor, (D) conductivity detector.

response for nitrate was determined to be linear over four decades (r = 0.9997) with a detection limit of 0.3 μm (S/N = 3).

All chromatographic data were collected by a 486 personal computer (IBM) interfaced with the potentiostat and conductivity detector by a DT2801 data acquisition board (Data Translation) and ASYST-3.1 software (Keithley/Asyst).

Treatment of data

Values of apparent heterogeneous rate constants (k_{app}, cm s^{-1}) for the anodic reaction of ethylamine and alanine were estimated from data obtained at the RDE from intercepts of linear plots of the reciprocal of the peak values of net current ($i_{p,net}^{-1}$, mA^{-1}) *vs.* the reciprocal square root of the rotational velocity ($\omega^{-1/2}$), according to the Koutecky-Levich equation:[5]

$$\frac{1}{i_{p,net}} = \frac{1}{n_{eff}FA_{geo}k_{app}C^b} + \frac{1}{0.62n_{eff}FA_{geo}D^{2/3}\upsilon^{-1/6}C^b\omega^{1/2}} \qquad (4)$$

where n_{eff} is the effective number of electrons in the reaction (eq mol^{-1}), A_{geo} is the geometric area of the disk electrode (cm^2), C^b is the bulk concentration of reactant (mol L^{-1}), υ is the kinematic viscosity of the solution (cm^2 s^{-1}), and F and D have their usual electrochemical significance.

Values of k_{app} for oxidation of NH_3 in the tubular, flow-through reactor were estimated according to:

$$k_{app} = (v_f/A_{tot})\log_e\{C^b_{NH_3,in}/C^b_{NH_3,out}\} \qquad (5)$$

where $C^b_{NH_3,in}$ and $C^b_{NH_3,out}$ represent the concentrations of NH_3 at the inlet and outlet of the

reactor, respectively; v_f is the volume flow rate ($cm^3\ s^{-1}$); and A_{tot} is the total area of the working electrode in the reactor (17.6 cm^2). Details of the derivation of Equation (5) are given in Appendix-A.

Results and Discussion

Ethylamine and alanine

The voltammetric response obtained for ethylamine and aquated ammonia at rotated disk electrodes (RDEs) constructed from an anodized Ag-Pb eutetic alloy has been described as a function of concentration and rotational velocity at ambient temperature.[1,2] For both reactants, plots of the background-corrected net current ($i_{net} = i_{tot} - i_{bkg}$) vs. potential are peak shaped for all concentrations and rotational velocities tested. This peak-shaped voltammetric response is interpreted as being a consequence of a bi-functional activity for the cationic silver sites in the anodized surface. More specifically, these sites are believed capable of adsorbing both the N-atoms in amine compounds as well as the O-atoms of hydroxyl species produced by anodic discharge of H_2O. Hence, at low values of applied overpotential, *i.e.*, low fluxes of the OH species, these sites function catalytically by adsorption of amine groups within the electrified interfacial region. However, at larger applied overpotentials, *i.e.*, high fluxes of the OH species, the majority of silver sites are occupied by adsorbed OH and the electrocatalytic mechanism for amine oxidation is blocked. With increasing flux of the reactant, *i.e.*, increasing concentration or rotational velocity, the peak in the net voltammetric response (i_{net}-E) is observed to be shifted to higher potentials.

Plots of the peak values of net current ($i_{p,net}$) made according to equation (3) were linear with non-zero intercepts. This is evidence that the reactions are under mixed control by heterogeneous kinetic and mass-transport processes.[5]

Shown in Figure 3.3 are typical voltammetric data illustrating the temperature sensitivity for the background current obtained in the absence of ethylamine (- - - -) as well as that for the total response in the presence of ethylamine (——) at a constant rotational velocity (168 rad s^{-1}). It is apparent that the i_{net}-E response is peak shaped in all cases illustrated. In fact, for $E > 1.1$ V (data not shown), $i_{tot} \propto i_{bkd}$ and, therefore, $i_{net} \propto 0$. Hence, there is no voltammetric evidence that oxidation of ethylamine can occur at an observable rate for large values of applied potential. Temperature in this study did not exceed 40 °C because of the volatility of ethylamine observed for $T > 40$ °C. The general shape of voltammetric curves obtained for alanine (not shown) are the same as represented in Figure 3.3 with a net voltammetric response (i_{net}-E) that exhibited a peaked shape.

Representative Koutecky-Levich plots for the net peak response ($i_{p,net}$) for 2.56 mM ethylamine and 2.0 mM alanine corresponding to 10 and 40 °C are shown in Figures 3.4 and 3.5, respectively. Linear regression statistics for all Koutecky-Levich plots are given in Tables 1 and 2 for ethylamine and alanine, respectively. In all cases, correlation coefficients (r) exceed values of 0.99 and the plots are concluded to be linear. Linearity of Koutecky-Levich plots is an indication that the value of n_{eff} is constant over the range of rotational velocities represented. However, values of the slopes for both ethylamine and alanine decrease dramatically as the temperature is increased. This is concluded to be an indication of increasing values of n_{eff} and these values, calculated on the basis of the generic values υ

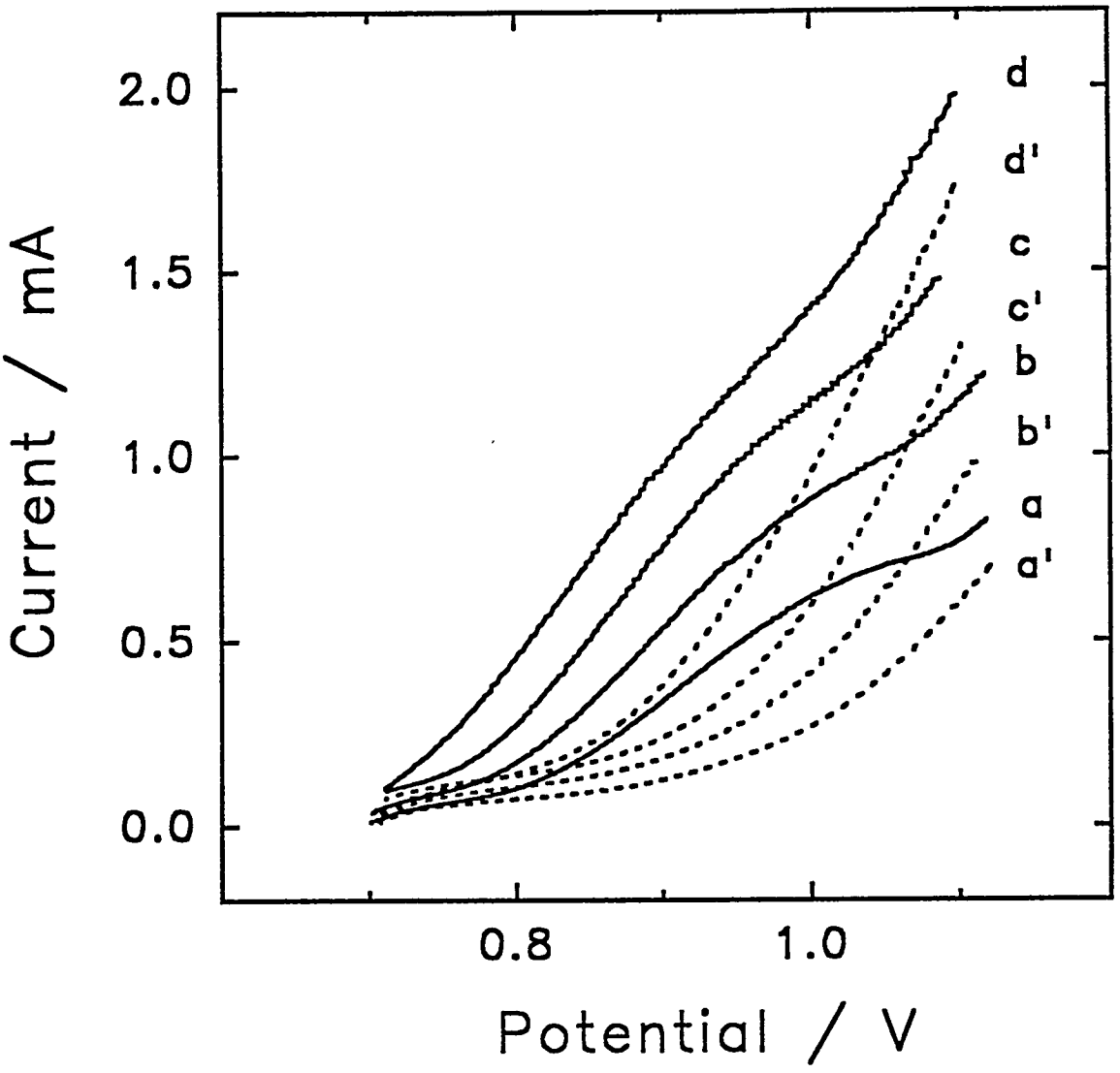

Figure 3.3. Voltammetric response for 2.0 mM ethylamine as a function of temperature in 1.0 M carbonate buffer (pH 10). Scan rate: 2.0 V min^{-1}. Rotation: 168 rad s^{-1}. Curves: (- - - -) residual, (——) ethylamine. Temperature (°C): (a,a') 10, (b,b') 20, (c,c') 30, (d,d') 40.

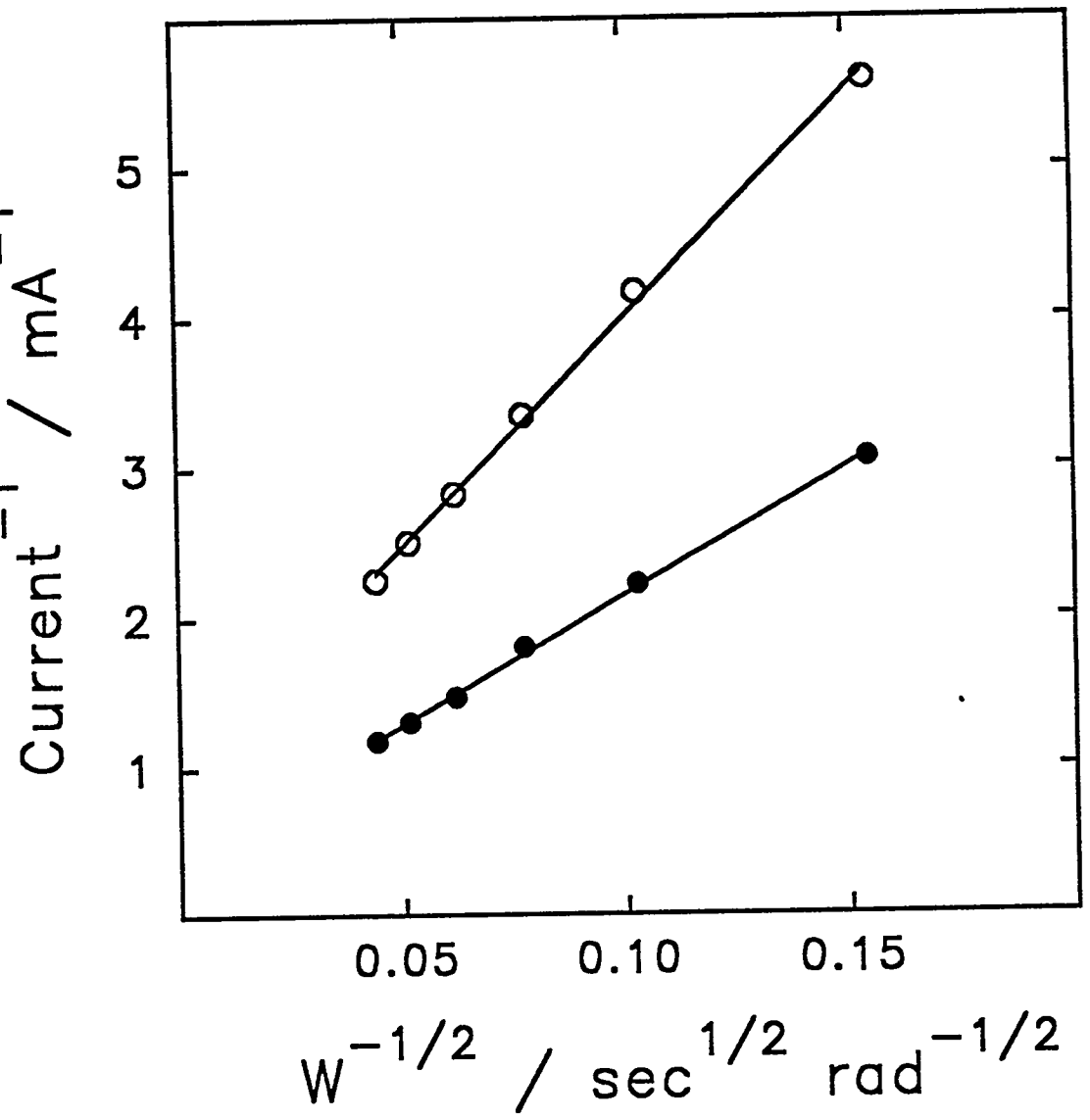

Figure 3.4. Representative Koutecky-Levich plots for 2.56 mM ethylamine in 1.0 M carbonate buffer (pH 10). Temperature (°C): (○) 10, (●) 40.

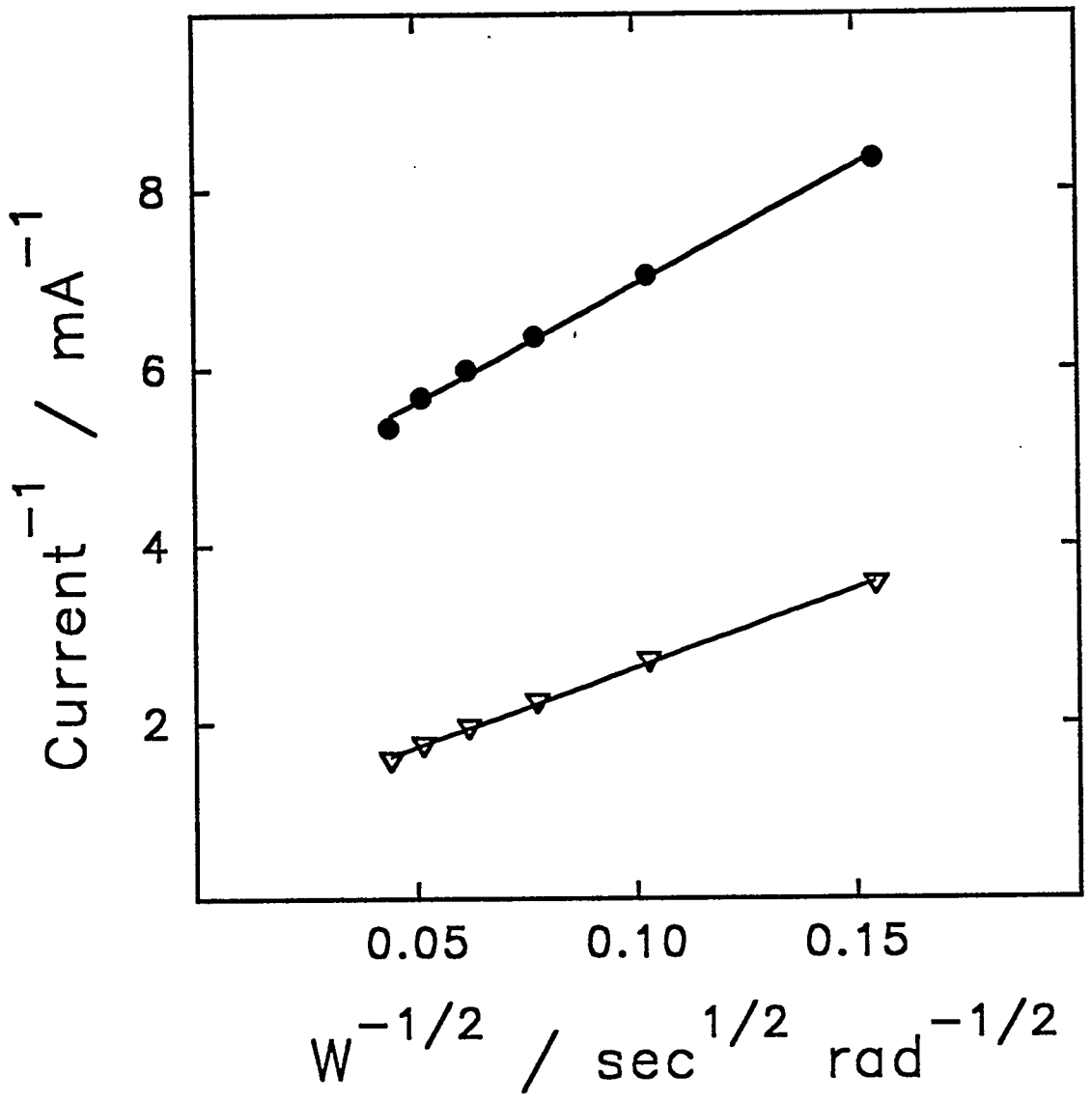

Figure 3.5. Representative Koutecky-Levich plots for 2.00 mM alanine in 1.0 M carbonate buffer (pH 10). Temperature (°C): (●) 10, (▽) 40.

= 0.010 $cm^2\ s^{-1}$ and D = $1.0x10^{-5}\ cm^2\ s^{-1}$, are given in the tables. The calculated values of n_{eff} at 20 °C are 1.9±0.1 eq mol^{-1} and 2.1±0.1 eq mol^{-1} for ethylamine and alanine, respectively. These values are in agreement with the value 2 eq mol^{-1} indicated in Equation (1) for oxidation of ethylamine determined in a previous study.[1] Also given in Tables 1 and 2 are values of k_{app} estimated from the intercepts using the calculated n_{eff} values.

Activation energies (ΔH°_{act}) for the peaked response of ethylamine and alanine were estimated from the slopes of Arrhenius plots of $\log\{k_{app}\}$ vs. $1/T$, using k_{app} values given in Tables 1 and 2. These Arrhenius plots are shown in Figures 3.6 and 3.7 for 2.56 mM ethylamine and 2.00 mM alanine, respectively. The corresponding slopes of the Arrhenius plots have the values $2.06x10^3$ and $8.62x10^2$ (°K) for ethylamine and alanine, respectively. From these slopes, the values of ΔH°_{act} are calculated to be 17.1 and 7.17 kJ mol^{-1} for ethylamine and alanine, respectively.

Ammonia

The high volatility of NH_3(aq) made it impractical to perform voltammetric studies of this reactant at elevated temperatures using the RDE in a conventional electrolysis cell. For this reason, the flow-through electrolytic reactor (Figure 3.1), coupled with an ion chromatograph (Figure 3.2), was used to determined the increase in the rate of NO_3^- production as a function of increasing temperature. Figure 3.8 shows the temperature dependent conversion of ammonia to nitrate within the flow-through system. The flow rate of the electrolyte was kept at only $8.2x10^{-3}\ cm^3\ s^{-1}$ (0.50 mL min^{-1}) to allow adequate thermal equilibration of the system. With temperature increasing from 14.5 to 52.0 °C the

Table 1. Statistics obtained from Koutecky-Levich plots for 2.56 mM ethylamine as a function of temperature in 1.0 M carbonate buffer (pH 10).

$$i_{p,net}^{-1} = a + b\omega^{-1/2}$$

Temperature (°C)	b (mA^{-1} $rad^{-1/2}$ $s^{1/2}$)	n_{eff} (eq mol^{-1})	a (mA^{-1})	$10^2 k_{app}$ [a] (cm s^{-1})
10	21.2	1.54	1.22	1.10
20	16.9	1.93	0.80	1.34
30	16.2	2.00	0.53	1.95
40	13.8	2.35	0.42	2.10

[a] Calculated from the intercept (a) using the n_{eff} value obtained from the slope (b).

$$\ln\{k_{app}\} = -2.06\text{x}10^3/T + 2.76$$

$$r = 0.976$$

$$\Delta H_{act} = 17.1 \text{ kJ mol}^{-1}$$

Table 2. Statistics obtained from Koutecky-Levich plots for 2.00 mM alanine as a function of temperature.

$$i_{p,net}^{-1} = a + b\omega^{-1/2}$$

Temperature (°C)	b (mA^{-1} $rad^{-1/2}$ $s^{1/2}$)	n_{eff} (eq mol^{-1})	a (mA^{-1})	$10^2 k_{app}$ [a] (cm s^{-1})
10	26.6	1.57	4.29	0.393
20	19.8	2.11	2.64	0.475
30	14.0	2.99	1.76	0.502
40	12.1	3.45	1.44	0.532

[a] Calculated from the intercept (a) using the n_{eff} value obtained from the slope (b).

$$\ln\{k_{app}\} = -8.62\text{x}10^2/\text{T} + 2.46$$

$$r = 0.956$$

$$\Delta H_{act} = 7.17 \text{ kJ mol}^{-1}$$

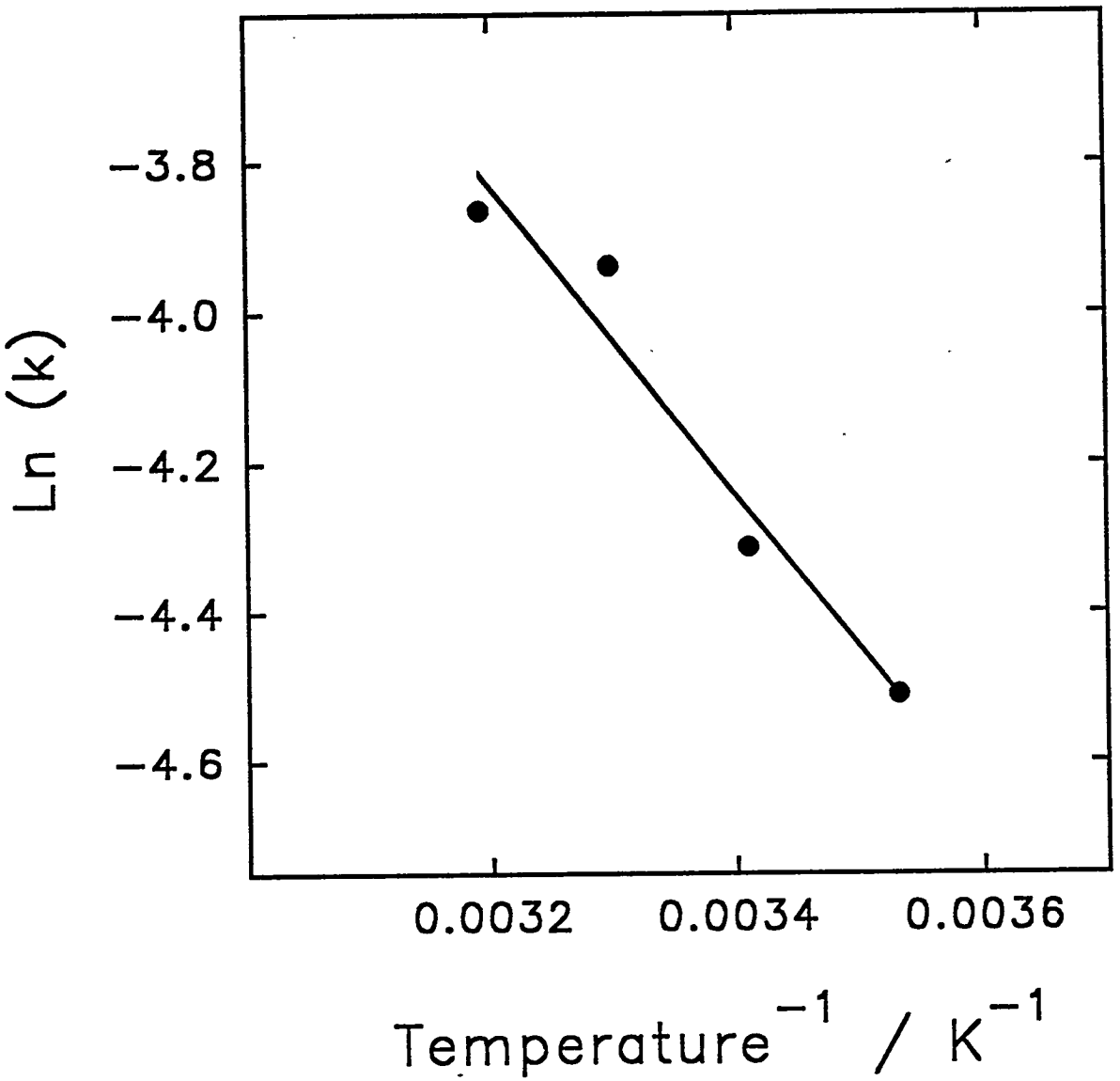

Figure 3.6. Arrhenius plot for 2.56 mM ethylamine in 1.0 M carbonate buffer (pH 10).

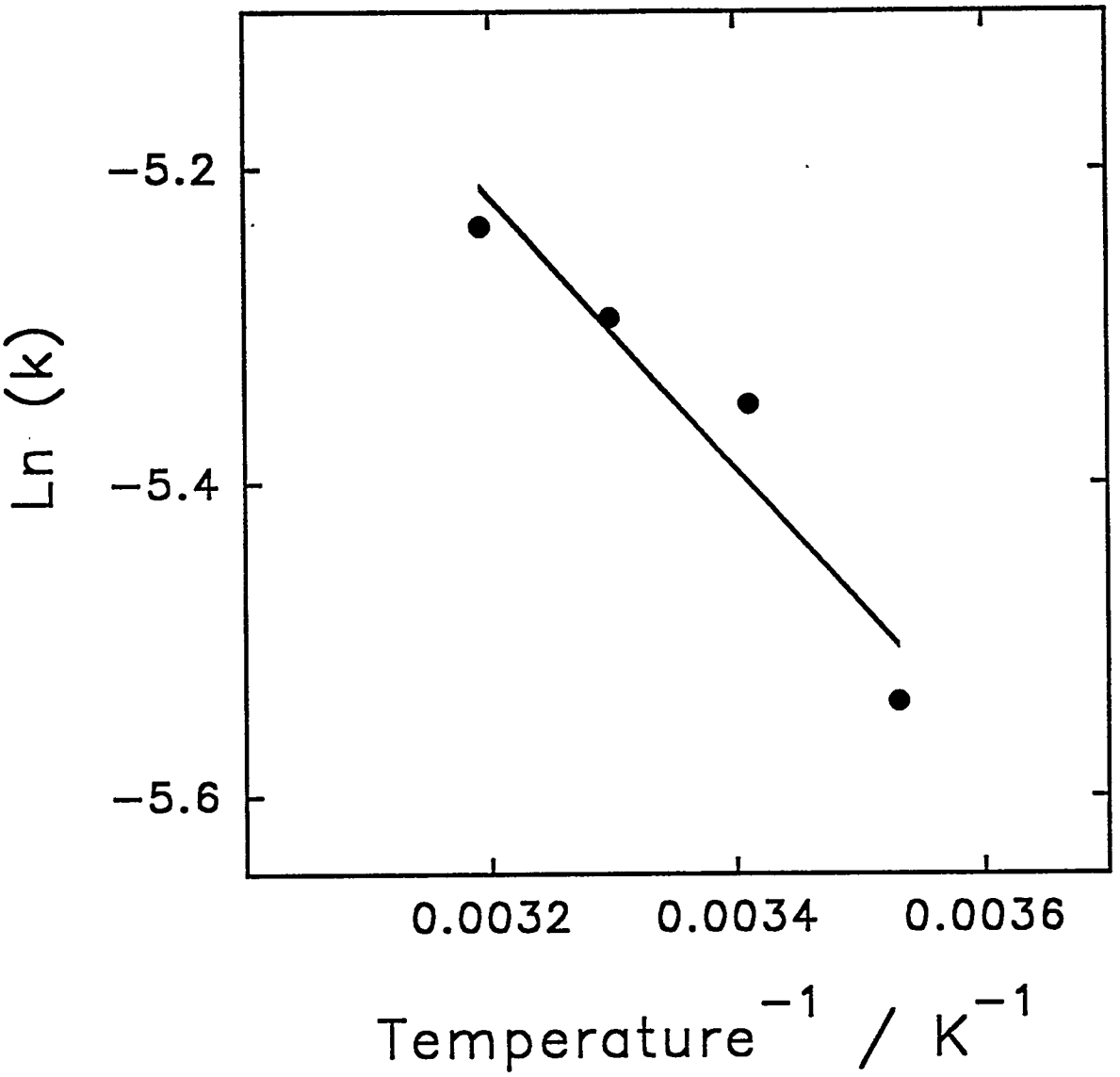

Figure 3.7. Arrhenius plot for 2.00 mM alanine in 1.0 M carbonate buffer (pH 10).

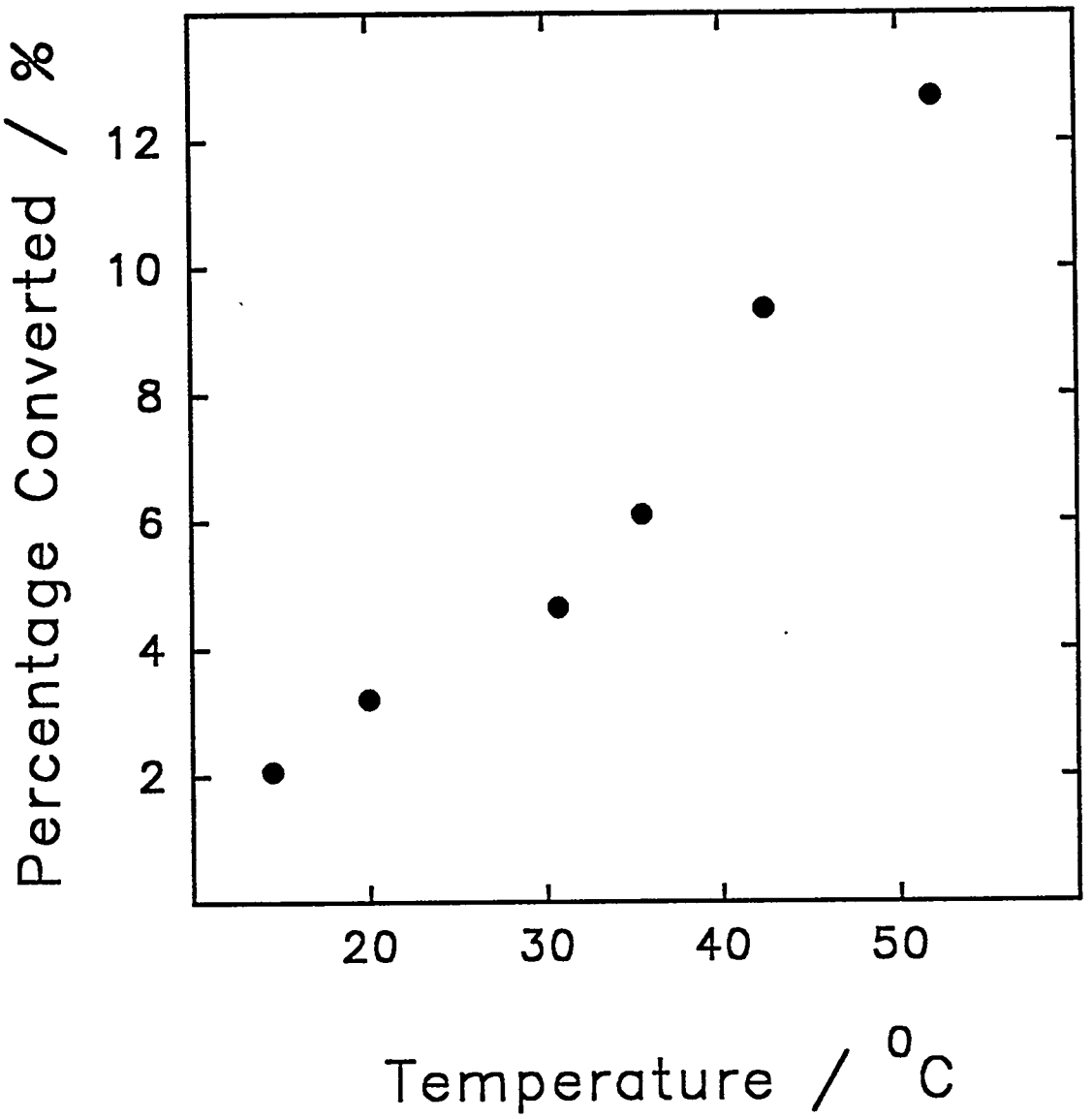

Figure 3.8. Percent conversion of total ammonia to nitrate ion in the flow-through reactor as a function of temperature. Flow rate: 8.2×10^{-3} cm^3 s^{-1} (0.50 mL min^{-1}).

percent conversion of NH_3(aq) to NO_3^- increased from 2.1 to 12.7%.

In the treatment of data from the flow-through reactor, it was assumed that the solvated NH_3, but not NH_4^+, is oxidized by a one-step mechanism according to:

$$NH_3 + 3H_2O \xrightarrow{k_{app}} NO_3^- + 9H^+ + 8e^- \quad (6)$$

where k_{app} is the apparent rate constant (cm s^{-1}) defined by:

$$\partial C^b_{NO_3^-}/\partial t = -\partial C^b_{NH_3}/\partial t = k_{app}(A/V)C^b_{NH_3} \quad (7)$$

where t is time (s), A is area of electrode surface, V is the volume of the electrolyte and C^b represents the bulk concentration of the indicated species. This assumption was concluded to be sufficient for this study based on chromatographic data showing NO_3^- as the only anionic product of electrolysis. Values of $C^b_{NH_3}$ in Equation (5) can be calculated from the bulk concentration of total ammonia ($C^b_{NH_4OH} = C^b_{NH_3} + C^b_{NH_4^+}$) on the basis of:

$$C^b_{NH_3} = f_{NH_3} C^b_{NH_4OH} \quad (8)$$

where f_{NH_3} is the fraction of the total ammonia that exists as NH_3, the electroactive species. However, the ratio $C^b_{NH_3,in}/C^b_{NH_3,out}$ in Equation (5) is independent of f_{NH_3} and can be calculated from experimental parameters according to:

$$\frac{C^b_{NH_3,in}}{C^b_{NH_3,out}} = \frac{f_{NH_3} C^b_{NH_4OH,in}}{f_{NH_3} C^b_{NH_4OH,out}} = \frac{C^b_{NH_4OH,in}}{C^b_{NH_4OH,in} - C^b_{NO_3^-,out}} \quad (9)$$

where $C^{b}_{NH_4OH,in}$ is the analytical concentration injected into the reactor and $C^{b}_{NO_3^-,out}$ is the NO_3^- concentration determined by ion chromatography at the reactor outlet.

Values of k_{app}, calculated from chromatographic data according to Equation (5), are given in Table 3 and plotted according to the Arrhenius equation in Figure 3.9. The slope of the Arrhenius plot is 4.6310^3 °K for which ΔH°_{act} for anodic oxidation of NH_3 is calculated to be 38.5 kJ mol^{-1}.

Variation of peak potentials

It continues to be a premise of this work that the anodic discharge of H_2O to form an adsorbed OH species is a prerequisite to the observed O-transfer reactions being studied. Hence, we expect that the minimum potential at which transport-limited oxidation of amine compounds is achieved will be increased as the flux of amines is increased. Therefore, it is expected also that peak potentials (E_p) observed for oxidation of amines at the Ag-Pb eutectic alloy electrodes will be shifted to higher potential values as a result of increased rotational velocity and/or amine concentration. For this approximate consideration, we assume that evolution of O_2 does not occur at a significant rate, i.e., the OH species are harvested solely by the amine oxidation mechanisms.

We assume a flux balance relating the rate of discharge of H_2O to produce OH and the rate of oxidation of reactant (R) at the peak potential ($E = E_p$), as given by:

$$Flux_{OH,p} = (n_{eff}/2)Flux_{R,p} \qquad (10)$$

where $n_{eff}/2$ is the number of O-atoms transferred in the oxidation of R. The flux of OH at

$E = E_p$ is assumed to be given by:

Table 3. Experimental results for NH_3 oxidation in flow-through reactor as a function of temperature. Conditions: $v_f = 8.2 \times 10^{-3}$ cm^3 s^{-1} (0.50 mL min^{-1}), $C^b_{NH_4OH,in}$ = 1.000 mM.

T (°C)	$C^b_{NO_3^-,out}$ (μM)	$\frac{C^b_{NH_3,in}}{C^b_{NH_3,out}} = \frac{C^b_{NH_4OH,in}}{C^b_{NH_4OH,in} - C^b_{NO_3^-,out}}$	$10^5 k_{app}$ [a] (cm s^{-1})
14.5	20.7	1.021	0.98
20.0	32.2	1.033	1.53
30.7	46.5	1.049	2.26
35.5	61.1	1.065	3.97
42.5	93.6	1.103	4.63
52.0	127	1.146	6.43

[a] Calculated from Equation (4).

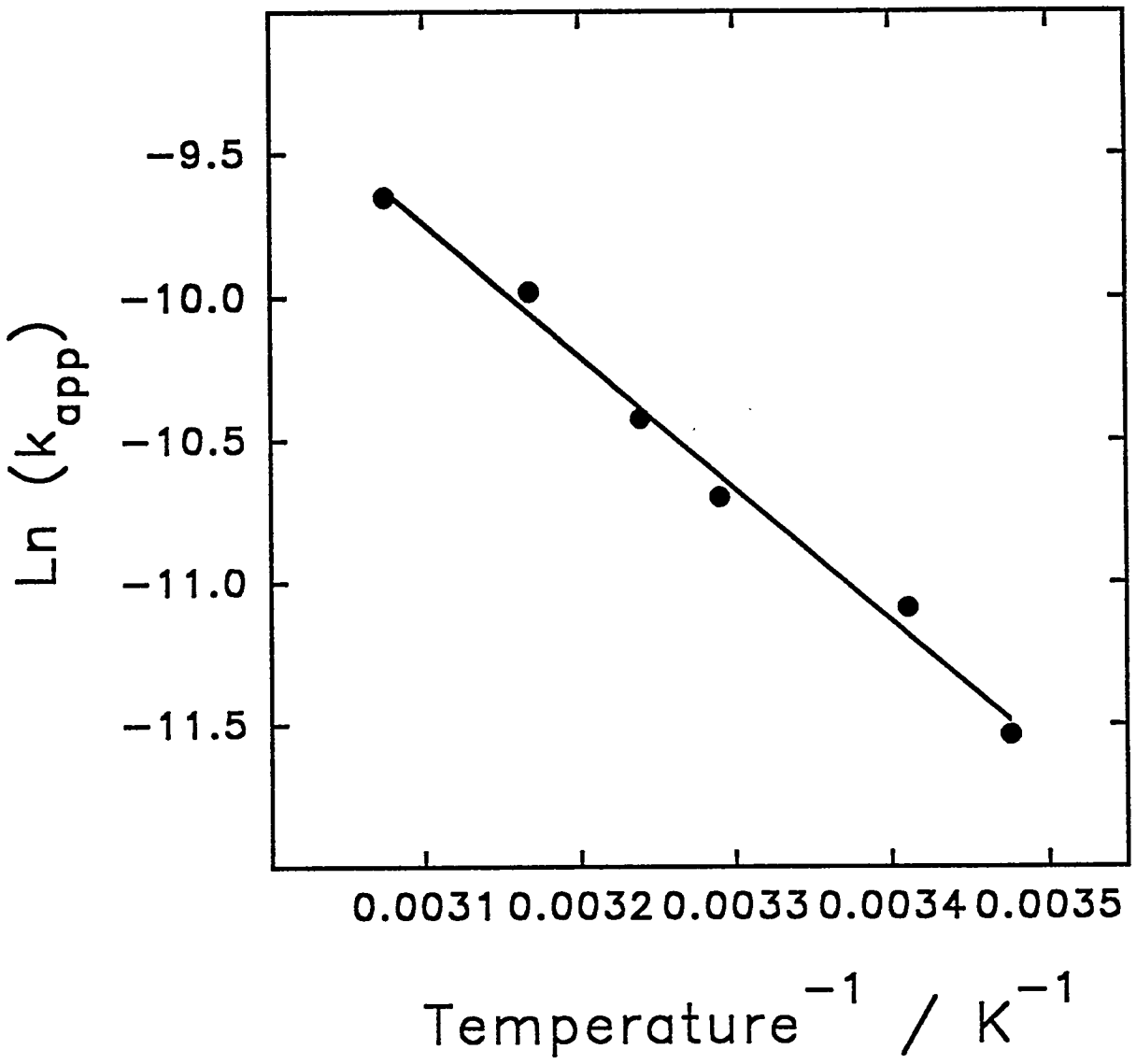

Figure 3.9. Arrhenius plot for oxidation of NH_3(aq) in flow-through reactor.

$$Flux_{OH,p} = \Gamma_{OH} A_{geo} k_o \exp\{\alpha F(E_p - E^{o'})/RT\} \quad (11)$$

where Γ_{OH} is the surface density of those sites capable of adsorbing OH (mol cm^{-2}); A_{geo} is the geometric area of the electrode; $E^{o'}$ is the formal reduction potential associated with the discharge of H_2O; and k_o and α are the heterogeneous rate constant and symmetry factor, respectively, for the anodic discharge of H_2O. We assume for $E = E_p$ that none of the silver sites are covered by adsorbed OH. The transport-limited flux of the reactant (R) at the RDE can be given by:

$$Flux_{R,p} = 0.62 A_{geo} D^{2/3} \upsilon^{-1/6} \omega^{1/2} C_R^b \quad (12)$$

where C_R^b is the bulk concentration of R (mol cm^{-3}). On the basis of Equations (11) and (12), we write:

$$\Gamma_{OH} A_{geo} k_o \exp\{\alpha F(E_p - E^{o'})/RT\} = (n_{eff}/2) 0.62 D^{2/3} \upsilon^{-1/6} \omega^{1/2} C_R^b \quad (13)$$

Solving Equation (13) for E_p gives:

$$E_p = E^{o'} + (RT/\alpha F)\ln\{0.62 n_{eff} D^{2/3} \upsilon^{-1/6}/2\Gamma_{OH} k_o\} + (RT/\alpha F)\ln\{\omega^{1/2} C_R^b\} \quad (14)$$

Assuming a constant value of n_{eff} we predict on the basis of Equation (14) that plots of E_p vs. $\ln\{\omega^{1/2}\}$ and vs. $\ln\{C_R^b\}$, for constant C_R^b and $\omega^{1/2}$, respectively, are linear with equivalent slopes, as indicated at 25 °C by:

$$\left(\partial E_p/\partial \ln\{\omega^{1/2}\}\right)_{C_R^b} = \left(\partial E_p/\partial \ln\{C_R^b\}\right)_{\omega^{1/2}} = RT/\alpha F = 0.0257/\alpha \quad (15)$$

The requirement of a transport-limited reaction at $E = E_p$ is satisfied most nearly in this study by the case of ethylamine. Plots of E_p vs. $\ln\{\omega^{1/2}\}$ and vs. $\ln\{C_R^b\}$ for ethylamine at 25 °C are shown in Figures 3.10 and 3.11. These plots are approximately linear, i.e., $r > 0.99$, and the slopes (and estimated α values) are 0.00825 (0.312) and 0.0378 (0.680), respectively.

Conclusion

The decrease in slopes of Koutecky-Levich plots for ethylamine and alanine observed as a result of increased temperature can come from: (i) decreased kinematic viscosity of the solution (υ), (ii) increased diffusion coefficients of the reactants (D), and (iii) increased values of the effective number of electrons (n_{eff}) in the electrode reaction. However, over the small range of temperatures tested, only dramatic changes in n_{eff} can explain the large changes in these slopes. The increase in n_{eff} values is indicative of an increased contribution to the electrode current from oxidation of NH_3 produced in the moderately fast initial step for oxidation of ethylamine and alanine. A consequence of the high temperature sensitivity for n_{eff} is the requirement of temperature control in analytical applications of anodized Ag-Pb eutectic electrodes, e.g., amperometric detection of amines following their separation by liquid chromatography. Furthermore, in this study, the variation of n_{eff} values makes a strict interpretation of ΔH°_{act} values even more problematic than is the usual case.

The anodic O-transfer reaction for ethylamine and alanine was confirmed to produce acetaldehyde and NH_3 at a rotated disk electrode at 25 °C; however, CO_2 is also a product

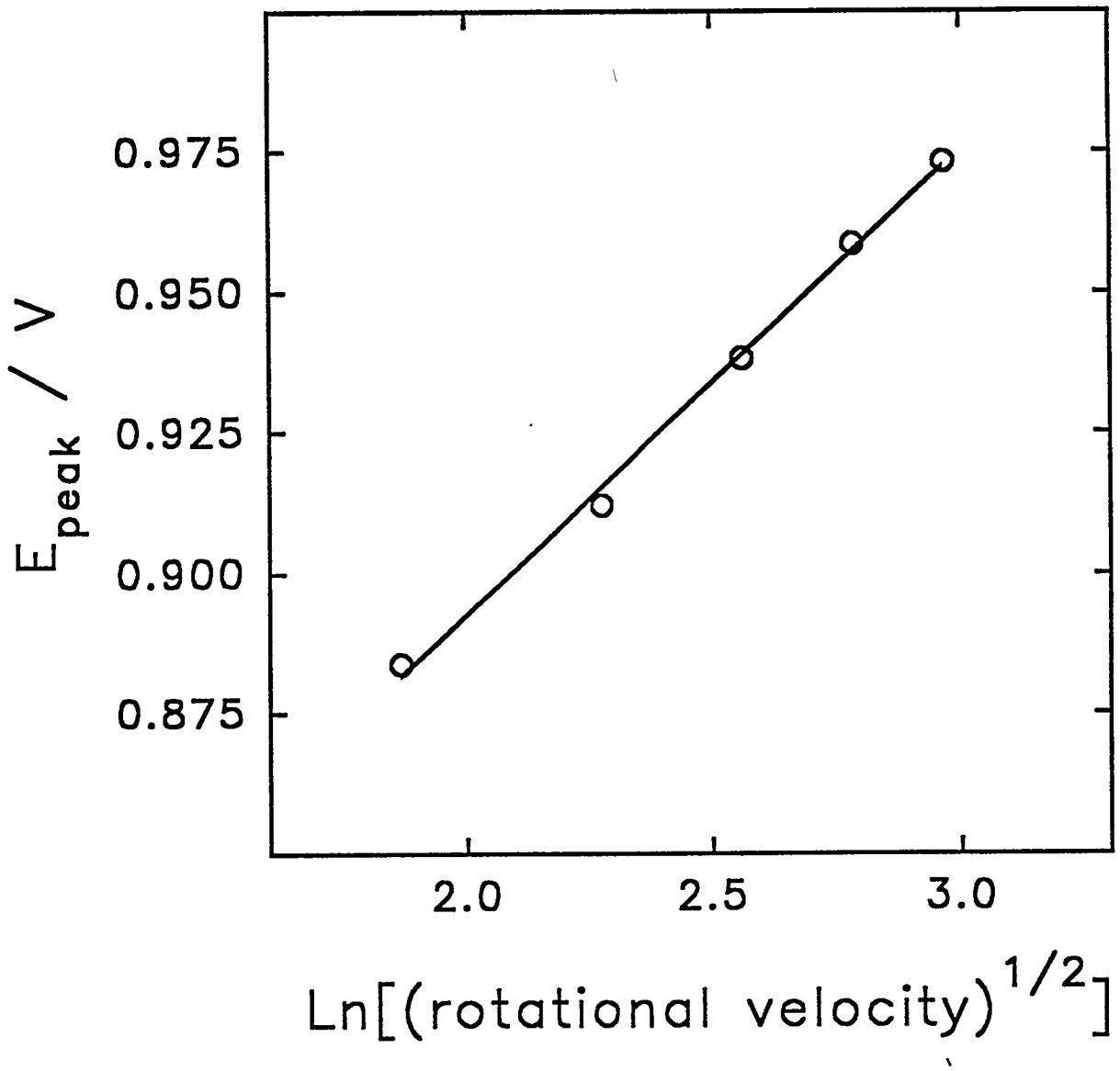

Figure 3.10. Correlation of peak potential for ethylamine with square root of rotational velocity in 1.0 M carbonate buffer (pH 10). Concentration: 2.50 mM.

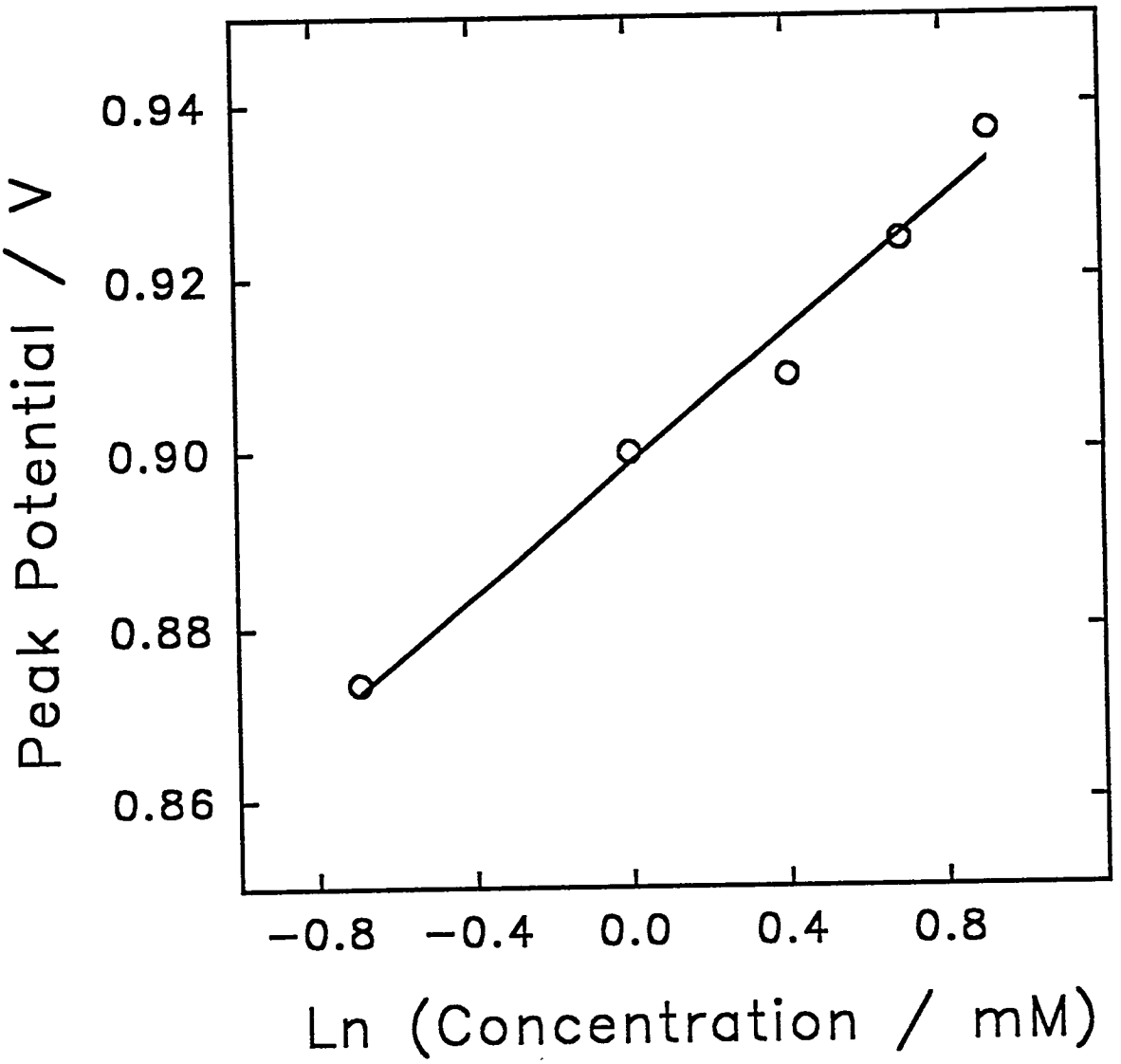

Figure 3.11. Correlation of peak potential for ethylene as a function of concentration in 1.0 M carbonate buffer (pH 10). Rotation: 168 rad s^{-1}.

of alanine oxidation.[1] These O-atom transfer steps are expected to proceed by the surface equivalent of a SN_2-type mechanism in which a non-bonded electron pair on OH_{ads} interacts with the anti-bonding orbital of the C-atom bonded to the adsorbed $-NH_2$ group. This is followed by oxidative dissociation of the H-atom from OH_{ads} and cleavage of the C-N bond with formation of NH_3. Such a surface mechanism requires the proximate location of adsorption sites for OH and $-NH_2$ as well significant vibrational motions of these adsorbed species along an axis passing through the O- and C-atoms. Values of ΔH°_{act} for oxidation of ethylamine and alanine are estimated to be 17.1 and 7.17 kJ mol^{-1}, respectively. Because the

$-COO^-$ group of alanine with this vibrational interaction. Future work is required to compare ΔH°_{act} and k_{app} values for a series of amino acids with systematically increasing distance between the $-NH_2$ and $-COO^-$ groups along a linear hydrocarbon chain.

The value of ΔH°_{act} determined for NH_3 oxidation is 38.5 kJ mol^{-1}. This large value is consistent with the very low value of k_{app} for this reaction and the observation that n_{eff} = ca. 2 eq mol^{-1} for ethylamine and alanine at the rotated disk electrode, i.e. no substantial contribution to total current from subsequent oxidation of NH_3 produced in the two-electron reaction. Hence, we conclude that the act of transferring an O-atom from OH_{ads} to adsorbed NH_3 is signficantly lower in probability than for O-transfer to the C-atom of ethylamine and alanine. If an SN_2-type mechanism of the sort described above also is operative for oxidation of NH_3 to NO_3^-, the direct interaction of adsorbed N- and O-atoms with the electrode surface can be expected to severly attenuate the vibrational motions that are necessary to achieve the transfer of the oxygen atom from OH_{ads} to the nearest $NH_{3,ads}$. Clearly, a detailed understanding is required of the local structural environment in the vicinity of adsorption sites for NH_3 and $-NH_2$, presumably at silver sites, and the OH species, presumable at adjacent lead sites, before the probabilities of various modes of O-atom transfer can be given even a qualitative evaluation.

The linear correlations observed between peak potential (E_p) for ethylamine oxidation and concentration, as well as rotational velocity of the electrode, is consistent with the assumption that an increased flux of the reactant requires an increased flux of the OH_{ads} species in the oxidation mechanism. Disagreement between the slopes of the E_p-ln$\{\omega^{1/2}\}$ and

E_p-ln$\{C^b\}$ plots is not understood at this time.

Appendix-A

The derivation of Equation (5) follows a similar derivation for a homogeneous reaction in a single-stage flow-through reactor.[6] It is assumed in this derivation that the contents of the reactor are well mixed in the cross section. Furthermore, because the rate of oxidation of NH_3 is very slow, the bulk and surface concentrations of NH_3 are assumed to be approximately equal, i.e., $C^s_{NH_3} = C^b_{NH_3}$. Accordingly, the relative change in $C^b_{NH_3}$ as a function of electrode area measured along the axis of the reactor is a function of the apparent heterogeneous rate constant (k_{app}) and the volume flow rate (v_f, $cm^3\ s^{-1}$) as given by:

$$\partial C^b_{NH_3}/C^b_{NH_3} = -(k_{app}/v_f)\partial A \qquad \text{(A-1)}$$

Equation (A-1) is integrated according to:

$$\int_{C^b_{NH_3,in}}^{C^b_{NH_3,out}} \partial C^b_{NH_3}/C^b_{NH_3} = -(k_{app}/v_f)\int_0^{A_{tot}} \partial A \qquad \text{(A-2)}$$

to give:

$$\log_e\{C^b_{NH_3,in}/C^b_{NH_3,out}\} = A_{tot}(k_{app}/v_f) \qquad \text{(A-3)}$$

where A_{tot} is the total electrode area, and $C^b_{NH_3,in}$ and $C^b_{NH_3,out}$ correspond to the concentration of NH_3 at the inlet and outlet, respectively, of the reactor. Equation (A-3) can be rearranged

to give Equation (5).

Acknowledgments

Ames Laboratory is operated for U.S. Department of Energy by Iowa State University under Contract No. W-7405-ENG-82.

References

1. J. Ge and D. C. Johnson, *This Journal*, **142**, 1525 (1995).

2. J. Ge and D. C. Johnson, *This Journal*, **142**, 3420 (1995).

3. B. S. Hui and C. O. Huber, *Anal. Chim. Acta*, **197**, 361 (1987).

4. Dionex, *Applications Notes*, No. 034217 (1990).

5. J. Koutecky and V. G. Levich, *Dokl. Akad. Nauk. SSSR*, **117**, 441 (1957); *Zh. Fiz. Khim.*, **32**, 1565 (1958).

6. C. D. Holland and R. G. Anthony, *Fundamentals of Chemical Reaction Engineering*, Prentice-Hall, Inc., Englewood Cliffs, New Jersey (1979) p.52.

GENERAL CONCLUSIONS

A novel electrocatalytic anode for oxidation of aliphatic amines has been found which consists of two synergetic oxide components: silver and lead. Design and fabrication of the electrode are based on the idea of incorporating finely dispersed catalytic active site such as silver oxide into an electrical conductive matrix such as lead oxide and the theoretic direction is proved to be valid and work by experimental results. Two methods have been used to manipulate the fabrication processes: (i) electrodeposition and (ii) anodizing of alloys. The electrodes prepared by electrodeposition of silver and lead oxides from Ag^{+} and Pb^{2+} carbonate buffer (pH 10) solution onto platinum substrate shown catalytic oxidation activity as voltammetry, amperometry and exhaustive electrolysis experimental indicated. The electrodeposited oxide layers were amorphous in nature as XRD indicated and were not bound to Pt substrate tight enough to prevent stripping loss when contact with different electrolytes. In sharp contract, oxide thin-film prepared by anodizing Ag-Pb alloys shown extraordinary stability in both physical appearance and observed current signals. Oxide surface structure determination of higher silver content by XRD shown that mixed oxides, namely AgO and litharge PbO were formed at anodized alloy surface. XPS analysis of the mixed oxide surface also proved that AgO was main component. Elemental mappings by EDS shown that big sized AgO islands were formed at alloys with higher silver content but totally absent at eutectic phase alloy electrode surface. The anodized alloy electrodes not only shown activity to primary amines, secondary, tertiary amines, but also alkaholamines and amino amino acids. The

electrode stability under constant applied potentials was tested by being mounted in a micro electrochemical detector cell connected with flow injection analysis (FIA) device. Typical data shown that for a long term flow injection-detection period the electrode behaved very stable when repeat contact with flux of ethylamine. For example, 45 hours continuous detection with injection rate of 5 min per injection results reproducible detection peak signals with relative standard deviation (RSD) of 4.7% and in each 5 hours period with RSD less than 1%. The detection sensitivity for most amines in flow electrolyte systems reaches picolmole level in general. The anodized eutectic Ag-Pb alloy electrode is particularly applicable in detection of aliphatic amines in flow electrolyte systems such as liquid chromatography systems.

It has been found that the electrode also shown oxidation activity for ammonia in alkaline solutions. Voltammetric experiment with pH change shown that maximum current observed for oxidation of ammonia was at pH around 9. Decreasing pH will decrease the oxidation current until its totally disappeared at pH below 4. This is explained by that deprotonation process is a prerequisite step so that the "nude" nitrogen atom with lone electron pairs can coordinately adsorbed onto electrode surface for achieving oxidation as mechanism promised. As pH increase to higher values, significant loss of ammonia due to volatility becomes a dominant factor and current peak decrease again. The anodic oxidation of ammonia is a relatively slow process as comparing with that of ethylamine which is characterized by heterogenous electron transfer rate constants calculated from Koutecky-Levich plots. Voltammetric experiment indicated that the oxidation of ammonia is a 8 eq mol^{-1} electron transfer process. Product identification in

exhaustive electrolysis solution of ammonia by more sophisticated techniques such as ion chromatography (IC) and nitrogen-15 NMR found that nitrate is the only product of the oxidation reaction. Same as ammonia, monitoring of electrolysis processes of the oxidation of amines such as ethylamine, methylethylamine, ethyldiamine, trimethylamine all shown increased nitrate signals in IC determinations. Therefore it is concluded that continuous oxidation of ammonia had happened in the oxidation of ethylamine with total electron transfer number of 10 eq mol^{-1}, but in the voltammetric experiments only a 2 eq mol^{-1} electron transfer process was observed in ambient condition with aldehyde and ammonia as main products.

The anodic process of oxidation of ammonia is proposed to be same as that of amines because of same peak shaped net current were observed in all cases. The electrode surface adsorbed hydroxyl radicals through water discharge was assured to plays a very important role such that at higher potentials oxygen evolution become significant which consumed most of the surface adsorbed hydroxyl radicals and blocked the oxygen transfer reactions.

The anodic oxidation of amines and ammonia at anodized Ag-Pb alloy electrodes are kinetically controlled reactions. It is expected that temperature will have profound effect on the oxidation rate, ie., the heterogenous electron transfer rate. For the purpose of estimating activation energy of extremely volatile ammonia, a device which permits monitoring nitrate product by ion chromatography from the continuous electrolysis oxidation of ammonia in elevated temperatures has be made and experiments proved it works well. The activation energies estimated from voltammetric experiments for

ethylamine and alanine and the activation energy of ammonia are significantly different from each other. It is thus concluded that rate determining step of the oxidation of amines is not electrode material related for the formation of hydroxyl radicals but rather reactants related. This rate determining step may involve many sub steps such as deprotonation, desolvation, surface adsorption, bond break and formation, desorption, solvation and protonation. It is difficult to point out which one of them is main contribution factor so far based on present data.

Peak shape is a general feature in net current observed for the oxidation of amines in voltammetric experiments. Peak potentials positive shifting with respect to the increase of electrode rotation velocity and reactant concentrations been explained by mathematic assumption that the flux of surface adsorbed hydroxyl radical formation rate is proportional to net current of oxidation of amines at peak values. The derivation of the mathematic assumption results linear relationships of peak potential to the logarithm of square root of rotational velocity and the logarithm of reactant bulk concentration which have been experimentally proved valid. The complexity of temperature effect on slope of the linear plots of Koutecky-Levich equation can been explained largely due to electron transfer number changes with increased contribution of slow succeeding reactions.

In summarization, electrocatalytic anodes have been discovered which show specific activity to amine containing aliphatic compounds. The anodized eutectic phase electrode is the most stable and sensitive anode which can be mechanically mounted in a flow electrolyte cell for purpose of detection of many aliphatic amines and amino acids in connection with liquid chromatography separation. The electrodes show complicated

oxidation pathways which is different in voltammetric and electrolysis experiments. The electron passed during oxidation processes can be increased with elevated temperatures. The surface hydroxyl radical formation is the prerequisite step for accomplishing oxygen transfer reactions but the limiting reaction for overall heterogenous electron transfer rate is perhaps the oxygen transfer reaction with specific reactants.

LITERATURE CITED

1. Martha Windholz, Susan Budavari, Lorraine Y. Stroumtsos, and Margaret Noether Fertig, *The Merk Index*, Ninth Edition, Merk & Co., Inc. (1976).
2. Carbide & Carbon Chemicals Corporation, Unit of Union Carbide & Carbon Corporation, *Organic Nitrogen Compounds*, 3, (1969).
3. ACS Symp. Ser., *Amine-Functionalized, Water-Soluble Polyamides as Drug Carriers*, **16** (Water-Soluble Polym.), 394, (1991).
4. Jurgen-Hinrich Fuhrhop, *Organic Synthesis: Concepts, Methods, Starting Materials*, 2nd ed, Weinheim, New York: VCH, (1994).
5. World Health Organization, *Ammonia*, **Environmental Health Criteria 54**, Geneva, (1986).
6. Thomas H. Chilton, *The Manufacture of Nitric Acid by the Oxidation of Ammonia: The Du Pont Pressure Process*, American Institute of Chemical Engineers, (1960).
7. Alan Townshend, *Encyclopedia of Analytical Science*, **5**, 2566 and 2592, (1995).
8. Margareta Avram, *Infrared Spectroscopy: Application in Organic Chemistry*, New York, Wiley-Interscience, (1972).
9. B. I. Ionin, *NMR Spectroscopy in Organic Chemistry*, New York, Plenum Press, 244, (1970).
10. J. R. Chapman, *Practical Organic Mass Spectrometry: A Guide for Chemical and Biochemical Analysis*, 2nd Ed., CHichester, New York: J. Wiley, 1993.
11. Boca Raton, *Amino Acids and Amines*, Fla.: CRC Press, (1983).

12. T. S. Ma, *Organic Functional Group Analysis by Gas Chromatographyh*, London, New York: Academic Press, (1976).

13. Kazutake Shimada, Tomoyuki OE, Makoto Tanaka and Toshio Nambara, *J. Chromatogr.*, **487**, 247, (1989).

14. Roger M. Smith and Asri Abdul Gbani, *Electroanalysis*, **2**, 167, (1990).

15. W. A. Jacobs and P. T. Kissiager, *J. Liq. Chromatogr.*, **5**, 881, (1982).

16. Laura A. Allison, Ginny S. Mager and Ronald E. SHoup, *Anal. Chem.*, **56**, 1089, (1984).

17. Chihiro Ueda, Kaoru Taninchi, Hidenobu Ohmori and Masaichiro Masui, *Anal. Sci.*, **3**, 377, (1987).

18. Karel Ŝtulĺk, Věra Paeákovâ, Kang Le and Bas Hennissen, *Talanta*, **35**, 455, (1988).

19. Peter W. Alexander and Carmelita Maitra, *Anal. Chem.*, **53**, 1590, (1981).

20. Karin Lsaksson, Jörgen Lindquist an Kent Lundström, *J. Chromatogr.*, **324**, 333, (1985).

21. Youqin Xie and Calvin O. Huber, *Anal. Chem.*, **63**, 1714, (1991).

22. A. R. Guadalupe, S. S. Jhareri, K. E. Liu, and H. D. Abruña, *Anal. Chem.*, **59**, 2436, (1987).

23. M. Nanjo and G. G. Guilbault, *Anal. Chim. Acta*, **73**, 367, (1974).

24. B. L. Wheeler, G. Caple, A. Henderson, J. Francis, K. Cantrell, S. Vogel, S. Grey and D. Russell, *J. Electrochem. Soc.*, **136**, 2769, (1989).

25. J. B. Kafil and C. O. Huber, *Anal. Chim. Acta*, **139**, 347, (1982).

26. W. Th. Kok, H. B. Hanekamp, P. Bos and R. W. Frei, *Anal. Chim. Acta*, **142**, 31, (1982).

27. Peifang Luo, Fuzhen Zhang and Richard P. Baldwin, *Anal. Chem.*, **63**, 1702, (1991).

28. Dennis C. Johnson and William R. LaCourse, *Electroanalysis*, **4**, 367, (1992).

29. C. K. Mann, Anal. Chem., 36, 2424, (1964).

30. C. K. Mann and K. A. Barnes, *Electrochemical Reactions in Non-Aqueous Systems*, Dekker, New York, 259, (1970).

31. N. L. Weinberg and H. R. Weinberg, *Chem. Rev.*, **68**, 475, (1968).

32. Y. Takayama, T. Harada and S. Miduno, *Bull. Chem. Soc., Japan*, **12**, 342, (1937).

33. K. A. Barnes and C. K. Mann, *J. Org. Chem.*, **32**, 1474, (1967).

34. Masaichiro Masui, Yoshiyuki Kamada, Taeko Iizuka and Shigeko Ozaki, *Chem. Pharm. Bull.*, **32**, 4740, (1984).

35. M. Fleishmann, K. Korinet and D. Pletcher, *J. Chem. Soc., Perkin Trans. II*, **10**, 1396, (1972).

36. N. A. Hampson, J. B. Lee, K. I. MacDonald, *Electrochim. Acta*, **17**, 921, (1972).

37. N. A. Hampson, J. B. Lee, J. R. Morley, K. I. MacDonald and B. Scanlon, *Tetrahedron*, **26**, 1109, (1970).

38. W. Boradman, G. Edwards, J. B. Lee, N. A. Hampson and K. I. MacDonald, *J. Electroanal. Chem.*, **33**, 95, (1971).

39. N. A. Hampson, J. B. Lee and K. I. MacDonald, *J. Electroanal. Chem.*, **34**, 91,

(1972).

40. J. S. Banait, S. Singh and P. K. Pahil, *J. Electrochem. Soc., India*, **33**, 173, (1984).

41. M. Fleischmann, K. Korinet and D. Pletcher, *J. Electroanal. Chem.*, **31**, 39, (1971).

42. H. J. Schäfer, *Topics Curr. Chem.*, **142**, 117, (1987).

43. P. Cox and D. Pletcher, *J. Appl. Electrochem.*, **21**, 11, (1991).

44. J. O'M. Bochris, *J. Chem. Phys.*, **24**, 817, (1956).

45. P. Rueschi and P. Delahay, *J. Chem. Phys.*, **23**, 556, (1955).

46. A. Damjanovic, A. Dey and J. O'M. Bockris, *Electrochim. Acta*, **11**, 791, (1966).

47. Y. Matsumoto, S. Yamada, T. Nishida and E. Sato, *J. Electrochem. Soc.*, **127**, 2360, (1980).

48. K. I. Rosenthal and V. I. Veselovskii, *Dokl. Akad. Nauk SSSR*, **111**, 637, (1956).

49. S. Trasatti, *J. Electroanal. Chem.*, **111**, 125, (1980).

50. T. Otagawa and J. O'M. Bockris, J. Electrochem. Soc., 129, 2391, (1982).

51. W. E. O'Grady, C. Iwakura and E. Yeager, *Am. Soc. Mech. Eng.*, **76-ENAS-37**, (1976).

52. A. G. C. Kobassen and G. H. J. Broers, *J. Electroanal. Chem.*, **126**, 221, (1981).

53. In-Hyeong Yeo, Sangsoo Kim, Robert Jacobson and Dennis C. Johnson, *J. Electrochem. Soc.*, **136**, 1395, (1989).

54. Joseph E. Vitt and Dennis C. Johnson, *J. Electrochem. Soc.*, **139**, 774, (1992).

55. Carol A. S. Brevett and Dennis C. Johnson, *J. Electrochem. Soc.*, **139**, 1314,

(1992).

56. Brian Wels and Dennis C. Johnson, *J. Electrochem. Soc.*, **137**, 2785, (1990).

57. J. Feng and Dennis C. Johnson, *J. Appl. Electrochem.*, **20**, 116, (1990).

58. J. Feng and Dennis C. Johnson, *J. Electrochem. Soc.*, **137**, 507, (1990).

59. J. Feng and Dennis C. Johnson, *J. Electrochem. Soc.*, **138**, 3328, (1991).

60. Jisheng Ge and Dennis C. Johnson, *J. Electrochem. Soc.*, **142**, 1525, (1995).

61. Jisheng Ge and Dennis C. Johnson, *J. Electrochem. Soc.*, **142**, 3420, (1995).

ACKNOWLEDGMENTS

I would like to express my gratitude to Dr. Johnson for support and guidance through my graduate studies. I was proud to work in Electrochemistry Group #1 under his detail oriented advising. With his patient disciplinary, bitter chemistry concepts, rigid scientific equations and harsh research activities become games full of fun, interesting and color.

I would also like to thank many former and present Johnson's group members. It was hard to forget that in my tough first year many former group members particularly Pete Vanderberg, James Gordon (Tiger as we called), Jiareng Feng and Rich Roberts helped me very much. I really benefit from many present group members through stimulating and helpful discussions and scientific presentations in group meetings. Kim Pamplin and I came to ISU in the same year and we went through everything all the way together in attending meetings, schedule study programs and so on and I will miss him very much.

Finally I would like to thank my family, particularly my parents, they gave me not only a beautiful life but also wisdom and philosophy heritage which guided me through my professional student years.

This work was performed at Ames Laboratory under Cotract No. W-7405-Eng-82 with the U.S. Department of Energy. The United States Government has assigned the DOE Report number IS-T1765 to this thesis.